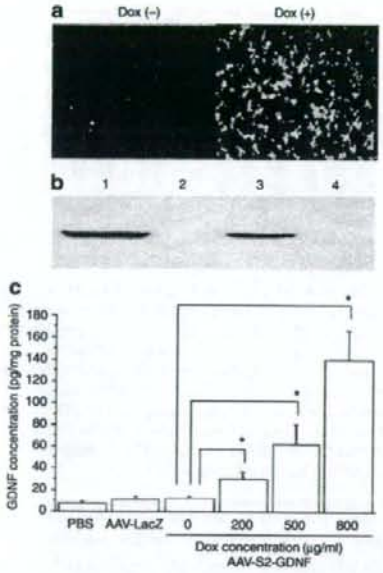


Figure 6 Induction of the transgene expression. (**a**) HEK293 cells were transfected with the proviral plasmid pAAV2-rtTA-S2-TRE-d2EGFP, and the expression of enhanced green fluorescent protein (EGFP) was induced by the doxycycline (Dox) (1 μg/ml). (**b**) Western blot analysis with an anti-FLAG antibody to detect the glial cell line–derived neurotrophic factor (GDNF) expression in the transduced 293 cells with the proviral plasmids. pAAV2-GDNF (lane 1), pAAV2-EGFP (lane 2), pAAV2-rtTA2s-S2-TRE-GDNF with Dox (lane 3), and pAAV2-rtTA2s-S2-TRE-GDNF without Dox (lane 4). (**c**) Dose–response of GDNF in the AAV2-S2-GDNF-injected muscle to the various concentrations of Dox. Mice were injected with phosphate-buffered saline (PBS), AAV2-LacZ, or AAV2-S2-GDNF followed by Dox administered in the drinking water. The mean muscle GDNF concentration in the animals treated with the AAV2-S2-GDNF in the absence of Dox was not significantly different compared to the animals treated with PBS or AAV2-*LacZ* ($P > 0.05$). The GDNF expression levels in the animals transduced with the AAV2-S2-GDNF significantly increased with increasing Dox concentration ($P < 0.05$). AAV1, adeno-associated virus 1.

In contrast, no detectable GDNF expression was observed in the cochlea of the AAV1-S2-GDNF/kanamycin group in the absence of Dox (data not shown).

## Protection of cochlear function with induced GDNF expression

To evaluate the adverse effects of the transduction procedure, ABR recordings were performed on kanamycin-free rats after injection of the inducible AAV1-S2-GDNF vectors and Dox administration. At all frequencies tested, no significant increase in the ABR threshold was observed after virus injection (**Figure 8a**). This result indicates that AAV1 vector injection, transgene expression, and Dox administration did not affect the ABR threshold of the experimental rats. Interestingly, even if AAV1-S2-GDNF was injected into the cochlea of one ear, the cochleas of both ears were protected in the presence of Dox. In particular, the ABR threshold shifts were significantly improved in both the AAV1-S2-GDNF-injected cochlea of the kanamycin-treated rats in the presence of Dox (**Figure 8b**)

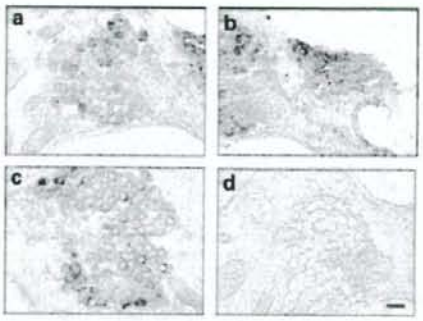


Figure 7 Expression of the GDNFflag in the rat cochlea. (**a, b, c**) The sections were sampled after the AAV1-S2-GDNF injection into the cochlea in the presence of doxycycline. GDNFflag expression was detected using an anti-FLAG antibody. (**d**) Samples from AAV1-EGFP-inoculated cochlea were analyzed as the negative control. Scale bar = 25 μm; ×400. AAV1, adeno-associated virus 1; GDNF, glial cell line–derived neurotrophic factor; EGFP, enhanced green fluorescent protein.

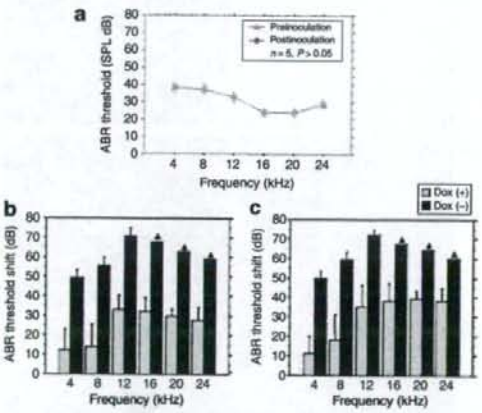


Figure 8 Protection of cochlear function with induced glial cell line–derived neurotrophic factor (GDNF) expression. (**a**) Auditory brain stem response (ABR) thresholds (mean ± SD) at each frequency tested in the AAV1-S2-GDNF-injected rat cochlea in the presence of doxycycline (Dox). No significant difference in the hearing thresholds was observed at each frequency between preinjection and postinjection. SPL, sound pressure level. ABR threshold shifts (mean ± SD) at each tested frequency in the (**b**) transduced or (**c**) nontransduced cochlea with or without Dox. Significant differences in the hearing threshold shifts were observed at each frequency between AAV1-S2-GDNF cochlea in the presence and absence of Dox ($n = 5$, $P < 0.05$). Arrows indicate the average ABR thresholds that exceeded the output power of the ABR apparatus.

and the cochlea of the noninjected contralateral ear (**Figure 8c**). However, the ABR threshold shifts at all frequencies were significantly lower in the treated group (AAV1-S2-GDNF/kanamycin plus Dox) than in the contralateral, untreated ear.

## DISCUSSION

In this study, we showed that both sustained and regulated AAV1-mediated GDNF expression protected the cochlear function of rats from aminoglycoside-induced ototoxicity. Indeed, damaged spiral ganglion cells and hair cells were significantly reduced by

regulated GDNF expression. The ABR monitoring revealed that there was no loss of the cochlear function over the frequencies tested after AAV vector injection and Dox treatment. These data suggest that regulated expression of GDNF in the cochlea efficiently preserves the cochlea from kanamycin-induced ototoxicity.

Among the various viral vector systems, the recombinant AAV-mediated gene transduction system offers several important advantages as a tool for direct somatic gene delivery into the cochlea. These include long-term stable expression of therapeutic genes in a wide variety of postmitotic tissues and minimal vector-related cytotoxicity.[26] In our previous report, we demonstrated the effective transduction of mouse cochleae with the AAV1-based vectors.[7] Generally the therapeutic effectiveness depends on an appropriate concentration and the half-life of the molecules. AAV vector–mediated gene transfer is a promising delivery technique to facilitate a long-term and chronic supply of therapeutic proteins that have a short half-life, such as GDNF. Furthermore, when the CAG promoter is used, efficient transduction activity is observed in the cochlear cells including the inner hair cells and spiral ganglion cells.[27,28]

Our data showed that AAV1-GDNF-mediated transduction of the rat cochleae provided significant protection of the cochlea against aminoglycoside-induced damage. This finding is consistent with previous studies that have used adenovirus-mediated GDNF expression[13,15,16] and demonstrates the feasibility of gene therapy with AAV1-based vectors for drug-induced hearing loss. Although the exact mechanism has not yet been elucidated, antioxidant pathways might be involved in the protective function of GDNF in the inner ear.[29] Free-radical formation following exposure to aminoglycoside is considered one of the major mechanisms to explain the aminoglycoside-related hair cell death.[1,30,31] It has been previously shown that GDNF is endogenously synthesized in the inner hair cells and spiral ganglion cells of the cochlea,[32] and the two known GDNF receptors are present in the spiral ganglion.[17,32,33] In the present study, we inoculated the cochlea with the AAV1 vectors via the round window membrane and detected a high level of transgene expression mainly in the inner hair cells and spiral ganglion cells. The AAV1-mediated GDNF expression pattern was similar to that of the endogenous protein; therefore GDNF supplemented *in situ* can play a substantial role in protection. Although the transduction of the *GDNF* gene was not observed in outer hair cells, GDNF levels in the perilymph of the manipulated cochleae was much higher than in the control cochleae. These cells may respond to the secretion of another growth factor that promotes hair cell survival. Upregulation of GDNF in inner hair cells and spiral ganglion cells following noise also support this concept.[34]

Compared to the vehicle controls, increased cochlear cell survival was observed in the contralateral ears of the AAV1-GDNF group, suggesting that the contralateral cochleae in treated rats were also moderately protected. Expression of the transgene was detected in the contralateral cochlea of the rats after injection with $5 \times 10^{10}$ genome copies of AAV1 per cochlea (data not shown). AAV can diffuse from one ear to the other via the cerebrospinal fluid in rodents.[35] Therefore, secreted GDNF molecules may also diffuse and exert a protective effect in the opposite ear. Alternatively, GDNF might enhance the neuronal activity (either afferent or efferent) of both ears, protecting both the treated and the contralateral cochlear function. Moreover, since infusion of the vectors into the cochlea forces large amounts of the vectors into the cerebrospinal fluid, any functional effect might be associated with the transduction of the brain. In this context, it is of great interest to know whether the otoprotective effect was achieved by the simple diffusion of the transgene product or direct transduction of the cells in the contralateral ear. To answer this question, we analyzed the local expression of the nonsecretory protein marker in the rodents with this transduction approach. Consequently, we feel that the direct transduction of the cells in the contralateral ear might be involved in the neuroprotection.

The present results showed that AAV-mediated delivery of a Tet-on system was able to control transgene expression. This Tet-on system incorporates the mutant transactivator rtTA2s-S2 and the transgene in which messenger RNA transcription is activated in the presence of an inducer, leading to protein expression. As we showed, the inducible expression of GDNF efficiently protected the cochlear structure and function from kanamycin-induced damage. GDNF was overexpressed in the induced state with the rtTA2s-S2 system, whereas GDNF expression was nearly normal in the non-induced state. In our study, cochlear function was significantly protected from aminoglycoside-induced cochlear damage in the presence of Dox. Although intracochlear injections did not affect physiological cochlear function, intramuscular injections of the vectors expressing Dox-dependent activators may elicit a cellular and humoral response against the transactivator in nonhuman primates.[36–38] The use of tissue-specific promoters that restrict transgene expression to nonprofessional antigen-presenting cells, and the use of AAV vectors, may reduce the induction of a specific T-cell response.[39]

Another attractive feature of the Tet-on system is the high safety profile of the inducer. In our study, Dox was orally administered to the rats to induce GDNF expression. Transgene expression levels were dependent on the dose of Dox, and the dose range of this inducer was below the normal bactericidal treatment levels used in similarly sized animals.[40,41] Furthermore, a Dox regimen in mice that is proportional to a clinically accepted dose of the drug in humans causes a significant induction of transgene expression.

Sequences of antibiotic administration and withdrawal to reverse the Dox induction of therapeutic gene expression were demonstrated in previous studies.[25,42] However, the aminoglycoside-induced hearing impairment model is not an appropriate model for adding and removing the Dox diet because the insulting phase is too short to successively induce and repress the Tet-on system. Furthermore, treatment of age-related hearing loss or genetic hearing loss ideally needs long-term gene expression studies to exclude any adverse events associated with the therapeutic genes.

Efficient control of the tetracycline-regulatory system is based on the specificity of the TetR/tetO interaction and the efficiency and safety of its inducers, such as tetracycline or Dox.[43,44] Mutant tTA2s are composed of one TetR and three repeated oligonucleotides of the VP-16-derived minimal activation domain. In the Tet-on system, rtTA2s-S2 showed a high activating ratio because its background expression level was lower than that of other mutants, such as rtTA2s-M2, which despite having a higher activation potential had also a high initial background.[25] By using the mutant transactivator, Urlinger *et al.* demonstrated that stringent regulation of target genes could be achieved over a range of four to five orders of magnitude

in stably transfected HeLa cells.[24] These regulatory systems could be further optimized to offer several potential advantages. The tetracycline-dependent transcriptional silencer allows tight regulation of transgene expression by eliminating baseline leakage.[20,45] Gene regulation mediated by rtTA2s-S2 was substantially tighter when combined with active silencing by the tetracycline-dependent transcriptional silencer in the non-induced state.[41,46]

Our results show that AAV1-mediated gene transfer is a promising gene delivery approach for the inner ear apparatus. To become an efficient and safe therapeutic method, it will be necessary to improve vector technology to achieve long-term transduction in a fail-safe system. We presented data demonstrating successful AAV-mediated transfer and modulation of transgene expression in the cochlea using a modified Tet-on system. In addition to the need for dosage control of neurotrophic factors, the AAV1 and the Tet-on system maybe useful for the regulation of the expression of other therapeutic gene products in the cochlea. Following further improvements, the rAAV-mediated transduction system may be of potential use for cochlear gene therapy applications in humans.

## MATERIALS AND METHODS

***Construction and preparation of the plasmids.*** The AAV vector proviral plasmid pAAV2-CAG-EGFP-WPRE (pAAV2-EGFP) contained the *EGFP* gene under the control of the CAG promoter and the WPRE and was flanked by inverted terminal repeats. A *Bam*HI fragment containing the GDNFflag complementary DNA was subcloned into this plasmid to obtain the pAAV2-CAG-GDNF-WPRE (pAAV2-GDNF) cassette.

The pAAV2-CMV-GDNFflag plasmid with the CMV promoter, the first intron of the human growth hormone gene, and the simian virus 40 polyadenylation signal sequence, were inserted between the inverted terminal repeats of the AAV type 2 genome.[47] The transactivator rtTA2s-S2 complementary DNA in the pUHrT61-1 plasmid (BD Biosciences, San Jose, CA) and the TRE in the pTRE-d2EGFP plasmid (BD Biosciences, CA) were subcloned together into the pAAV2-CMV-GDNFflag plasmid to obtain the AAV vector proviral plasmid pAAV2-rtTA2s-S2-TRE-GDNF. A *Sac*II-*Eco*RI fragment containing the d2EGFP complementary DNA from the pTRE-d2EGFP plasmid (BD Biosciences, CA) was subcloned into this plasmid to create the pAAV2-rtTA2s-S2-TRE-EGFP plasmid (see **Supplementary Materials and Methods**).

***Recombinant AAV vector production.*** The AAV1 vectors were produced as previously described by using a 293-cell transfection protocol[26] with the proviral plasmid pAAV2-EGFP, pAAV2-Luciferase,[48] pAAV2-GDNF, pAAV2-rtTA2s-S2-TRE-EGFP, or pAAV2-rtTA2s-S2-TRE-GDNF; the AAV packaging plasmid pAAV1RepCap; and the adenovirus helper plasmid pAdeno5 using an active gassing system.[49] The recombinant AAV2 expressing the *Escherichia coli* $\beta$-galactosidase gene under the control of the CMV promoter (AAV2-LacZ) was generated using the proviral plasmid pAAV-LacZ.[50] (see **Supplementary Materials and Methods**).

**In vitro *expression of GDNF.*** To detect the *in vitro* expression of the GDNFflag fusion protein, 293 cells were transduced with the AAV1-GDNFflag at $1 \times 10^4$ vector genome copies/cell. For the detection of the regulated expression, 293 cells were transduced with the AAV proviral plasmid pAAV2-rtTA2s-S2-TRE-d2EGFP or pAAV2-rtTA2s-S2-TRE-GDNF in the presence or absence of 1 μmol/l Dox-HCl (Sigma, St Louis, MO) (see **Supplementary Materials and Methods**).

***Surgical procedures and cochlear perfusions.*** All animal studies were performed in accordance with the guidelines issued by the committee on animal research at Jichi Medical University. Twenty 5-week-old male Sprague–Dawley rats with normal Preyer's reflexes weighing 130–150 g were utilized (CLEA Japan, Tokyo, Japan). Five-week-old male C57BL/6J mice were utilized for optical bioluminescence imaging. The animals were anesthetized with ketamine (50 mg/kg) and xylazine (5 mg/kg). A postauricular approach was performed to expose the tympanic bony bulla. A small opening (2 mm in diameter) to the tympanic bulla was made by carefully drilling through the bone of the bulla to gain access to the round window membrane. Subsequently, 5 μl of AAV vector solution (AAV1-EGFP, AAV2-Luciferase, or AAV1-GDNF, $5 \times 10^{10}$ genome copies, $n = 5$ each) was microinjected into the cochlea through the round window for over 10 minutes using a glass micropipette (40 μm in diameter) fitted on a Univentor 801 syringe pump (Serial No. 170182, High Precision Instruments, Univentor Ltd., Malta). The rats were also injected with the AAV1-S2-GDNF in the presence ($n = 5$) or absence ($n = 5$) of Dox. A small plug of muscle was used to seal the cochlea, and the surgical wound was closed in layers and dressed with an antibiotic ointment.

***Transgene expression* in vivo.** The rats were deeply anesthetized and the perilymph was sampled from the inoculated cochlea through the round window. GDNF protein levels were measured using a GDNF Emax ImmunoAssay System (Promega, Madison, WI) according to the manufacturer's instructions. The GDNF expression in the rat cochlea was determined by immunohistochemistry using an anti-FLAG antibody.

AAV2-LacZ or AAV2-S2-GDNF vector ($1 \times 10^{10}$ genome copies) was injected into the quadriceps of the C57BL/6J mice (6 weeks old, CLEA Japan, Tokyo, Japan). The mice were injected with phosphate-buffered saline ($n = 5$) or AAV2-*LacZ* ($n = 5$). Animals treated with various concentrations of Dox were injected with the AAV2-S2-GDNF ($n = 5$ per group). Two weeks after the transduction, animals were deeply anesthetized, and the injected muscle was sampled. The tissue levels of the GDNF protein were measured with an enzyme-linked immunosorbent assay kit (GDNF Emax ImmunoAssay System, Promega, WI), according to the manufacturer's instructions. The levels of GDNF were expressed as pg/mg protein. The assay sensitivity ranged from 16 to 1,000 pg/ml.

Two weeks after the injection of the AAV2-Luciferase, optical bioluminescence imaging was performed using the CCD camera (Xenogen, Alameda, CA). After intraperitoneal injection of reporter substrate D-Luciferin (375 mg/kg body weight), mice were imaged for scans.

***Kanamycin administration and ABR assessment.*** A dose of 333 mg of kanamycin base/kg body weight was obtained by injecting 3 μl/g body weight. Seven days after virus injection, kanamycin was given subcutaneously twice daily for 12 consecutive days. The body weight of the animals was monitored daily to adjust the kanamycin dosages accordingly.

Auditory thresholds were determined by audiometry of evoked ABRs using Tucker-DAVIS Technologies and Scope software (Power Lab; ADInstruments, Coloado Springs, CO). Thresholds were evaluated for each animal prior to the start of the injection procedure and 2 days after the termination of kanamycin treatment. The ABRs were measured as previously described,[7] using a two-way repeated analysis of variance (see **Supplementary Materials and Methods**).

***Histological evaluation of the cochlear preservation.*** Cochlear hair cell loss was determined by F-actin staining. One month after transduction, the presence of the cochlear spiral ganglion neurons was determined by 4′,6-diamino-2-phenylindole dihydrochloride staining to visualize nuclear chromatin. After decalcification, 6 μm mid-modiolus cryosections of the cochleae from each animal were histologically analyzed. The number of spiral ganglion neurons was determined in every third section of the cochlear basal turn from the AAV1-transduced and kanamycin-treated rats (see **Supplementary Materials and Methods**).

***Statistical analyses.*** Results are presented as the means ± SD. Data were statistically analyzed using analysis of variance, paired student's *t*-test (injected versus contralateral sides) or unpaired student's *t*-test (therapy versus control groups) (StatView 5.0 software; SAS Institute, Cary, NC).

## ACKNOWLEDGMENTS

The authors thank Avigen. (Alameda, CA) for providing the pAAV-LacZ and pAdeno. We also thank Thomas Hope (Department of Microbiology and Immunology, The University of Illinois at Chicago) for providing pBS II SK+WPRE-B11 and Jun-Ichi Miyazaki (Osaka University Graduate School of Medicine, Osaka, Japan) for pCAGGS. The authors also thank Miyoko Mitsu for her encouragement and technical support. This work was supported in part by grants from the Ministry of Health, Labour and Welfare of Japan (Grants-in-Aid for Scientific Research and grant for 21 Century Centers of Excellence program) and the "High-Tech Research Center" Project for Private Universities (matching fund subsidy, from the Ministry of Education, Culture, Sports, Science, and Technology of Japan). The authors declare no conflict of interest.

## SUPPLEMENTARY MATERIAL

**Materials and Methods.**

**Figure S1.** Bioluminescence of the transduced cochlea in living mice.

## REFERENCES

1. Wu, WJ, Sha, SH and Schacht, J (2002). Recent advances in understanding aminoglycoside ototoxicity and its prevention. *Audiol Neurootol* **7**: 171–174.
2. Hellier, WP, Wagstaff, SA, O'Leary, SJ and Shepherd, RK (2002). Functional and morphological response of the stria vascularis following a sensorineural hearing loss. *Hear Res* **172**: 127–136.
3. Tsue, TT, Oesterle, EC and Rubel, EW (1994). Hair cell regeneration in the inner ear. *Otolaryngol Head Neck Surg* **111**: 281–301.
4. Raphael, Y, Frisancho, JC and Roessler, BJ (1996). Adenoviral-mediated gene transfer into guinea pig cochlear cells *in vivo*. *Neurosci Lett* **207**: 137–141.
5. Ishimoto, S, Kawamoto, K, Kanzaki, S and Raphael, Y (2002). Gene transfer into supporting cells of the organ of Corti. *Hear Res* **173**: 187–197.
6. Okada, T, Nomoto, T, Shimazaki, K, Ujun, W, Lu, Y, Matsushita, T *et al.* (2002). Adeno-associated virus vectors for gene transfer to the brain. *Methods* **28**: 237–247.
7. Liu, Y, Okada, T, Sheykholeslami, K, Shimazaki, K, Nomoto, T, Muramatsu, SI *et al.* (2005). Specific and efficient transduction of cochlear inner hair cells with recombinant adeno-associated virus type 3 vector. *Mol Ther* **12**: 725–733.
8. Lin, LF, Doherty, DH, Lile, JD, Bektesh, S and Collins, F (1993). GDNF: a glial cell line-derived neurotrophic factor for midbrain dopaminergic neurons. *Science* **260**: 1130–1132.
9. Henderson, CE, Phillips, HS, Pollock, RA, Davies, AM, Lemeulle, C, Armanini, M *et al.* (1994). GDNF: a potent survival factor for motoneurons present in peripheral nerve and muscle. *Science* **266**: 1062–1064.
10. Wang, Y, Lin, SZ, Chiou, AL, Williams, LR and Hoffer, BJ (1997). Glial cell line-derived neurotrophic factor protects against ischemia-induced injury in the cerebral cortex. *J Neurosci* **17**: 4341–4348.
11. Keithley, EM, Ma, CL, Ryan, AF, Louis, JC and Magal, E (1998). GDNF protects the cochlea against noise damage. *Neuroreport* **9**: 2183–2187.
12. Shoji, F, Yamasoba, T, Magal, E, Dolan, DF, Altschuler, RA and Miller, JM (2000). Glial cell line-derived neurotrophic factor has a dose dependent influence on noise-induced hearing loss in the guinea pig cochlea. *Hear Res* **142**: 41–55.
13. Suzuki, M, Yagi, M, Brown, JN, Miller, AL, Miller, JM and Raphael, Y (2000). Effect of transgenic GDNF expression on gentamicin-induced cochlear and vestibular toxicity. *Gene Ther* **7**: 1046–1054.
14. Yagi, M, Kanzaki, S, Kawamoto, K, Shin, B, Shah, PP, Magal, E *et al.* (2000). Spiral ganglion neurons are protected from degeneration by GDNF gene therapy. *J Assoc Res Otolaryngol* **1**: 315–325.
15. Hakuba, N, Watabe, K, Hyodo, J, Ohashi, T, Eto, Y, Taniguchi, M *et al.* (2003). Adenovirus-mediated overexpression of a gene prevents hearing loss and progressive inner hair cell loss after transient cochlear ischemia in gerbils. *Gene Ther* **10**: 426–433.
16. Kawamoto, K, Yagi, M, Stover, T, Kanzaki, S and Raphael, Y (2003). Hearing and hair cells are protected by adenoviral gene therapy with TGF-beta1 and GDNF. *Mol Ther* **7**: 484–492.
17. Kuang, R, Hever, G, Zajic, G, Yan, Q, Collins, F, Louis, JC *et al.* (1999). Glial cell line-derived neurotrophic factor. Potential for otoprotection. *Ann NY Acad Sci* **884**: 270–291.
18. Yagi, M, Magal, E, Sheng, Z, Ang, KA and Raphael, Y (1999). Hair cell protection from aminoglycoside ototoxicity by adenovirus-mediated overexpression of glial cell line-derived neurotrophic factor. *Hum Gene Ther* **10**: 813–823.
19. Meng, X, Lindahl, M, Hyvonen, ME, Parvinen, M, de Rooij, DG, Hess, MW *et al.* (2000). Regulation of cell fate decision of undifferentiated spermatogonia by GDNF. *Science* **287**: 1489–1493.
20. Perez, N, Pience, P, Millet, V, Greuet, D, Minot, C, Noel, D *et al.* (2002). Tetracycline transcriptional silencer tightly controls transgene expression after *in vivo* intramuscular electrotransfer: application to interleukin 10 therapy in experimental arthritis. *Hum Gene Ther* **13**: 2161–2172.
21. Regulier, E, Pereira de Almeida, L, Sommer, B, Aebischer, P and Deglon, N (2002). Dose-dependent neuroprotective effect of ciliary neurotrophic factor delivered via tetracycline-regulated lentiviral vectors in the quinolinic acid rat model of Huntington's disease. *Hum Gene Ther* **13**: 1981–1990.
22. Rubinchik, S, Woraratanadharm, J, Yu, H and Dong, JY (2005). New complex Ad vectors incorporating both rtTA and tTS deliver tightly regulated transgene expression both *in vitro* and *in vivo*. *Gene Ther* **12**: 504–511.
23. Pluta, K, Luce, MJ, Bao, L, Agha-Mohammadi, S and Reiser, J (2005). Tight control of transgene expression by lentivirus vectors containing second-generation tetracycline-responsive promoters. *J Gene Med* **7**: 803–817.
24. Urlinger, S, Baron, U, Thellmann, M, Hasan, MT, Bujard, H and Hillen, W (2000). Exploring the sequence space for tetracycline-dependent transcriptional activators: novel mutations yield expanded range and sensitivity. *Proc Natl Acad Sci USA* **97**: 7963–7968.
25. Lamartina, S, Roscilli, G, Rinaudo, CD, Sporeno, E, Silvi, L, Hillen, W *et al.* (2002). Stringent control of gene expression *in vivo* by using novel doxycycline-dependent trans-activators. *Hum Gene Ther* **13**: 199–210.
26. Okada, T, Shimazaki, K, Nomoto, T, Matsushita, T, Mizukami, H, Urabe, M *et al.* (2002). Adeno-associated viral vector-mediated gene therapy of ischemia-induced neuronal death. *Methods Enzymol* **346**: 378–393.
27. Stone, IM, Lurie, DI, Kelley, MW and Poulsen, DJ (2005). Adeno-associated virus-mediated gene transfer to hair cells and support cells of the murine cochlea. *Mol Ther* **11**: 843–848.
28. Liu, Y, Okada, T, Nomoto, T, Ke, X, Kume, A, Ozawa, K *et al.* (2007). Promoter effects of adeno-associated viral vector for transgene expression in the cochlea *in vivo*. *Exp Mol Med* **39**: 170–175.
29. Oppenheim, RW (1997). Related mechanisms of action of growth factors and antioxidants in apoptosis: an overview. *Adv Neurol* **72**: 69–78.
30. Priuska, EM and Schacht, J (1995). Formation of free radicals by gentamicin and iron and evidence for an iron/gentamicin complex. *Biochem Pharmacol* **50**: 1749–1752.
31. Sha, SH and Schacht, J (1999). Stimulation of free radical formation by aminoglycoside antibiotics. *Hear Res* **128**: 112–118.
32. Sanicola, M, Hession, C, Worley, D, Carmillo, P, Ehrenfels, C, Walus, L *et al.* (1997). Glial cell line-derived neurotrophic factor-dependent RET activation can be mediated by two different cell-surface accessory proteins. *Proc Natl Acad Sci USA* **94**: 6238–6243.
33. Ylikoski, J, Pirvola, U, Virkkala, J, Suvanto, P, Liang, XQ, Magal, E *et al.* (1998). Guinea pig auditory neurons are protected by glial cell line-derived growth factor from degeneration after noise trauma. *Hear Res* **124**: 17–26.
34. Nam, YJ, Stover, T, Hartman, SS and Altschuler, RA (2000). Upregulation of glial cell line-derived neurotrophic factor (GDNF) in the rat cochlea following noise. *Hear Res* **146**: 1–6.
35. Kho, ST, Pettis, RM, Mhatre, AN and Lalwani, AK (2000). Safety of adeno-associated virus as cochlear gene transfer vector: analysis of distant spread beyond injected cochleae. *Mol Ther* **2**: 368–373.
36. Favre, D, Blouin, V, Provost, N, Spisek, R, Porrot, F, Bohl, D *et al.* (2002). Lack of an immune response against the tetracycline-dependent transactivator correlates with long-term doxycycline-regulated transgene expression in non-human primates after intramuscular injection of recombinant adeno-associated virus. *J Virol* **76**: 11605–11611.
37. Latta-Mahieu, M, Rolland, M, Caillet, C, Wang, M, Kennel, P, Mahfouz, I *et al.* (2002). Gene transfer of a chimeric trans-activator is immunogenic and results in short-lived transgene expression. *Hum Gene Ther* **13**: 1611–1620.
38. Lena, AM, Giannetti, P, Sporeno, E, Ciliberto, G and Savino, R (2005). Immune responses against tetracycline-dependent transactivators affect long-term expression of mouse erythropoietin delivered by a helper-dependent adenoviral vector. *J Gene Med* **7**: 1086–1096.
39. Cordier, L, Gao, GP, Hack, AA, McNally, EM, Wilson, JM, Chirmule, N *et al.* (2001). Muscle-specific promoters may be necessary for adeno-associated virus-mediated gene transfer in the treatment of muscular dystrophies. *Hum Gene Ther* **12**: 205–215.
40. McGee Sanftner, LH, Rendahl, KG, Quiroz, D, Coyne, M, Ladner, M, Manning, WC *et al.* (2001). Recombinant AAV-mediated delivery of a tet-inducible reporter gene to the rat retina. *Mol Ther* **3**: 688–696.
41. Lamartina, S, Silvi, L, Roscilli, G, Caslmiro, D, Simon, AJ, Davies, ME *et al.* (2003). Construction of an rtTA2(s)-m2/tts(kid)-based transcription regulatory switch that displays no basal activity, good inducibility, and high responsiveness to doxycycline in mice and non-human primates. *Mol Ther* **7**: 271–280.
42. Srour, MA, Fechner, H, Wang, X, Siemetzki, U, Albert, T, Oldenburg, J *et al.* (2003). Regulation of human factor IX expression using doxycycline-inducible gene expression system. *Thromb Haemost* **90**: 398–405.
43. Kistner, A, Gossen, M, Zimmermann, F, Jerecic, J, Ullmer, C, Lubbert, H *et al.* (1996). Doxycycline-mediated quantitative and tissue-specific control of gene expression in transgenic mice. *Proc Natl Acad Sci USA* **93**: 10933–10938.
44. Knott, A, Garke, K, Urlinger, S, Guthmann, J, Muller, Y, Thellmann, M *et al.* (2002). Tetracycline-dependent gene regulation: combinations of transregulators yield a variety of expression windows. *Biotechniques* **32**: 796, 798, 800 passim.
45. Rendahl, KG, Quiroz, D, Ladner, M, Coyne, M, Seltzer, J, Manning, WC *et al.* (2002). Tightly regulated long-term erythropoietin expression in vivo using tet-inducible recombinant adeno-associated viral vectors. *Hum Gene Ther* **13**: 335–342.
46. Salucci, V, Scarito, A, Aurisicchio, L, Lamartina, S, Nicolaus, G, Giampaoli, S *et al.* (2002). Tight control of gene expression by a helper-dependent adenovirus vector carrying the rtTA2(s)-M2 tetracycline transactivator and repressor system. *Gene Ther* **9**: 1415–1421.
47. Wang, L, Muramatsu, S, Lu, Y, Ikeguchi, K, Fujimoto, K, Okada, T *et al.* (2002). Delayed delivery of AAV-GDNF prevents nigral neurodegeneration and promotes functional recovery in a rat model of Parkinson's disease. *Gene Ther* **9**: 381–389.
48. Okada, T, Uchiborl, R, Iwata-Okada, M, Takahashi, M, Nomoto, T, Nonaka-Sarukawa, M *et al.* (2006). A histone deacetylase inhibitor enhances recombinant adeno-associated virus-mediated gene expression in tumor cells. *Mol Ther* **13**: 738–746.
49. Okada, T, Nomoto, T, Yoshioka, T, Nonaka-Sarukawa, M, Ito, T, Ogura, T *et al.* (2005). Large-scale production of recombinant viruses by use of a large culture vessel with active gassing. *Hum Gene Ther* **16**: 1212–1218.
50. Okada, T, Mizukami, H, Urabe, M, Nomoto, T, Matsushita, T, Hanazono, Y *et al.* (2001). Development and characterization of an antisense-mediated prepackaging cell line for adeno-associated virus vector production. *Biochem Biophys Res Commun* **288**: 62–68.

Neurobiology of Aging 29 (2008) 574–585

# Selective loss of nigral dopamine neurons induced by overexpression of truncated human α-synuclein in mice

Masaki Wakamatsu, Aiko Ishii, Shingo Iwata, Junko Sakagami, Yuriko Ukai, Mieko Ono, Daiji Kanbe, Shin-ichi Muramatsu, Kazuto Kobayashi, Takeshi Iwatsubo, Makoto Yoshimoto

Reprinted from NEUROBIOLOGY OF AGING, Vol. 29, No. 4, April 2008

ELSEVIER

Neurobiology of Aging 29 (2008) 574–585

NEUROBIOLOGY OF AGING

www.elsevier.com/locate/neuaging

# Selective loss of nigral dopamine neurons induced by overexpression of truncated human α-synuclein in mice☆

Masaki Wakamatsu[a], Aiko Ishii[a], Shingo Iwata[a], Junko Sakagami[a], Yuriko Ukai[a], Mieko Ono[a], Daiji Kanbe[a], Shin-ichi Muramatsu[b], Kazuto Kobayashi[c], Takeshi Iwatsubo[d], Makoto Yoshimoto[a,*]

[a] *Medicinal Research Laboratories, Taisho Pharmaceutical Co., Ltd., Yoshino-cho 1-403, Kita-ku, Saitama-shi, Saitama 331-9530, Japan*
[b] *Division of Neurology, Department of Medicine, Jichi Medical University, Shimotsuke-shi, Tochigi 329-0498, Japan*
[c] *Department of Molecular Genetics, Institute of Biomedical Sciences, Fukushima Medical University School of Medicine, Fukushima-shi, Fukushima 960-1295, Japan*
[d] *Department of Neuropathology and Neuroscience, Graduate School of Pharmaceutical Sciences, University of Tokyo, Bunkyo-ku, Tokyo 113-0033, Japan*

Received 18 July 2006; received in revised form 4 October 2006; accepted 16 November 2006
Available online 14 December 2006

**Abstract**

Parkinson's disease is characterized by loss of nigral dopaminergic neurons and presence of Lewy bodies, whose major component is α-synuclein. In the present study, we generated transgenic mice termed Syn130m that express truncated human α-synuclein (amino acid residue number: 1–130) in dopaminergic neurons. Notably, dopaminergic neurons were selectively diminished in the substantia nigra pars compacta of Syn130m, while transgenic mice that expressed comparable amount of full-length human α-synuclein did not develop such pathology. Therefore, the truncation of human α-synuclein seems to be primarily responsible for the loss of nigral dopaminergic neurons. The nigral pathology resulted in impairment of axon terminals in the striatum and concomitant decrease in striatal dopamine content. Behaviorally, spontaneous locomotor activities of Syn130m were reduced, but the abnormality was ameliorated by treatment with L-DOPA. The loss of nigral dopaminergic neurons was not progressive and seemed to occur during embryogenesis along with the onset of expression of the transgene. Our results indicate that truncated human α-synuclein is deleterious to the development and/or survival of nigral dopaminergic neurons.


*Keywords:* Parkinson's disease; Animal model; α-Synuclein; Transgenic mouse; Tyrosine hydroxylase; Dopamine neuron

## 1. Introduction

Parkinson's disease (PD) is the second most common neurodegenerative disorder clinically characterized by a variety of motor dysfunctions such as bradykinesia, rigidity, resting tremor and postural abnormalities. These symptoms are attributed to the reduction of striatal dopamine (DA) level, which results from selective and progressive degeneration of DAergic neurons in the substantia nigra pars compacta (SNc). Recent studies have demonstrated that point mutations, Ala53Thr (A53T), Ala30Pro and Glu46Lys, in the α-synuclein gene and triplication of a chromosomal region spanning the α-synuclein gene are individually responsible for the onset of autosomal dominant PD in several pedigrees (Kruger et al., 1998; Polymeropoulos et al., 1997; Singleton et al., 2003; Zarranz et al., 2004). In addition, it has been reported that α-synuclein is a major structural component of Lewy bodies (LBs), which are cytoplasmic inclusions and pathological hallmarks of PD (Arawaka et al., 1998; Arima et

*Abbreviations:* DA, dopamine; H&E, hematoxylin and eosin; LB, Lewy body; PD, Parkinson's disease; SNc, substantia nigra pars compacta; Tg, transgenic; TH, tyrosine hydroxylase; VTA, ventral tegmental area

☆ Kazuto Kobayashi and Takeshi Iwatsubo received grants from Taisho Pharmaceutical Co., Ltd.

* Corresponding author. Tel.: +81 48 669 3095; fax: +81 48 652 7254.
*E-mail address:* m.yoshimoto@po.rd.taisho.co.jp (M. Yoshimoto).

0197-4580/$ – see front matter © 2006 Elsevier Inc. All rights reserved.
doi:10.1016/j.neurobiolaging.2006.11.017

al., 1998; Baba et al., 1998; Spillantini et al., 1998; Takeda et al., 1998; Wakabayashi et al., 1997). The above background strongly suggests that α-synuclein plays an important role in the pathogenesis of PD.

α-Synuclein is a presynaptic protein composed of 140 amino acid residues and was first discovered as the precursor protein of non-Aβ component of Alzheimer's disease amyloid or NACP (Iwai et al., 1995; Ueda et al., 1993). Accumulating evidence indicates that at least a part of α-synuclein in LBs is truncated from the C-terminus (Baba et al., 1998; Campbell et al., 2001; Liu et al., 2005; Tofaris et al., 2003), and that C-terminal truncation accelerates aggregation of α-synuclein in vitro (Crowther et al., 1998; Du et al., 2003; Murray et al., 2003). In addition, a recent report indicates that the C-terminal truncation of α-synuclein is a normal cellular process (Liu et al., 2005). These data imply that aberrant truncation of α-synuclein has some relevance to the pathogenesis of PD. However, it is not clear at this stage if the processing is actually involved in the development of the disease.

To examine the in vivo function of truncated α-synuclein, we generated transgenic (Tg) mice that express the C-terminally truncated α-synuclein carrying an A53T point mutation under the control of the rat tyrosine hydroxylase (TH) promoter, which enables the transgene to be expressed in DAergic neurons. The truncation was determined to be 10 amino acid residues for the following reasons: (1) Truncation by 10 residues kept the epitope for LB509 (amino acid residue number: 115–122), a monoclonal antibody which discriminates between human α-synuclein and mouse α-synuclein (Jakes et al., 1999). Therefore, expression of the transgene was readily and specifically detected by using LB509. (2) Recombinant α-synuclein with the deletion formed aggregates much faster than full-length α-synuclein in vitro. (3) Ser129, which is mainly phosphorylated in LBs (Fujiwara et al., 2002), was retained in truncated α-synuclein. Thus, the possible involvement of this modification in the phenotype of Tg mice could be investigated.

Remarkably, there was a considerable and selective loss of DAergic neurons in the SNc of the Tg mice. In addition, the Tg mice showed behavioral abnormality which was rectified by the administration of L-DOPA, the most commonly used drug to treat PD. Thus, the Tg mice of the present study developed some of the typical symptoms of PD.

## 2. Materials and methods

### 2.1. Construction of TH-α-synuclein transgenes

A DNA fragment containing the 9-kb 5′-flanking region of the rat TH gene was prepared by digesting pTH/-9 kb (Iwawaki et al., 2000) with *Xho*I and *Hin*dIII, and inserted into pBST-N (Kobayashi et al., 1992) to construct pRTH-BstN. A cDNA fragment encoding human α-synuclein was prepared by reverse transcription-polymerase chain reaction (RT-PCR) using human brain RNA as a template, and a point mutation, GCA (Ala53) → ACA (Thr53), was introduced into the gene. A cDNA fragment (1.2 kb) containing the α-synuclein(A53T) gene was inserted into the *Eco*RI site of pRTH-BstN, resulting in a recombinant plasmid, pRTH-Syn140m. Another PCR was carried out to introduce a stop codon just after the 130th residue of human α-synuclein(A53T) by using pRTH-Syn140m as a template and the following oligonucleotides as primers: 5′-ggaattcattagccatggatgtattc and 5′-tagccttaagttactcagaaggcattt. The resultant DNA fragment (417 bp) was similarly inserted into pRTH-BstN to construct pRTH-Syn130m.

### 2.2. Generation of Tg mice

The recombinant plasmids were digested with *Sal*I, and transgene constructs of 12.2 kb (pRTH-Syn140m) and 11.5 kb (pRTH-Syn130m) were purified (Fig. 1a). The constructs were individually microinjected into the pronuclei of fertilized eggs of B6C3F1 hybrid according to the standard procedure (Hogan et al., 1994). Offspring were screened for the transgene by PCR analysis of DNA extracted from tail biopsies using the following primer set: 5′-gtggctgctgctgagaaaac (P1) and 5′-gtggggctccttcttcattc (P2). Each founder mouse was backcrossed with C57BL/6J mice, and all subsequent studies were performed with N4 or later generations. Tg mice at 8 weeks of age and age-matched non-Tg littermates were analyzed in this study unless otherwise mentioned. All the animal experiments reported here were carried out in accordance with guidelines of the Japanese Association for Laboratory Animal Science.

### 2.3. Immunoblot analysis

The midbrain and the striatum of adult mice were dissected in consultation with the respective brain maps (Paxinos and Franklin, 2001). The coordinates measured from the interaural line were as follows: from 6.0 to 2.0 mm for the striatum, and from 2.0 to −1.6 mm for the midbrain. The cortex and the hippocampus were removed from the midbrain sections. Cytoplasmic fractions prepared from the brain sections were subjected to immunoblot analysis according to the method described previously (Wakabayashi et al., 1997). The primary antibodies used for the analysis were LB509 (1:750 dilution), a mouse monoclonal antibody that specifically recognizes human α-synuclein (Zymed Laboratories, South San Francisco, CA), NACP5 (1:5000 dilution), a rabbit polyclonal antibody that reacts with both human and mouse α-synuclein and does not crossreact with β-synuclein (Wakabayashi et al., 2000), a rabbit anti-NSE antibody (1:1000 dilution; Polysciences, Warrington, PA) and a rabbit anti-TH antibody (1:400 dilution; Novus Biologicals, Littleton, CO). The intensities of the bands were quantified with ImageMaster 1D Elite (Amersham Biosciences, Tokyo, Japan).

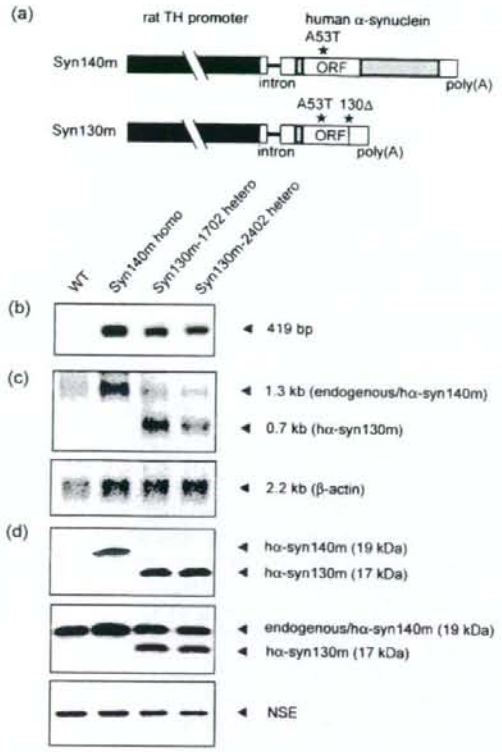


Fig. 1. Expression of the transgenes: (a) Schematic structures of the transgene constructs used to generate Syn140m and Syn130m mice. The constructs contain the rat TH promoter (closed box), the second intron of rabbit β-globin gene, open reading frame (ORF) of the human α-synuclein gene, and an SV40 poly(A) addition signal. Gray boxes indicate 5′- and 3′-untranslated regions of the gene. (b) Southern blot analysis. Genomic DNAs (10 μg) extracted from tail biopsies of Tg mice (heterozygous Syn130m-1702 and Syn130m-2402, and homozygous Syn140m mice) and age-matched non-Tg littermates (WT) were digested with *Eco*RI, electrophoresed, and transferred onto a membrane. The membrane was incubated with a digoxigenin (DIG)-labeled α-synuclein probe prepared by PCR using pRTH-Syn140m as a template and P1 and P2 (see Section 2.2) as primers. (c) Northern blot analysis. Poly(A)$^+$ RNAs (4 μg) extracted from the whole brain were electrophoresed and transferred onto a membrane. The membrane was hybridized with the DIG-labeled α-synuclein probe (upper panel), dehybridized, and reprobed with a DIG-labeled β-actin cDNA (lower panel). (d) Immunoblot analysis. Cytoplasmic proteins (50 μg) prepared from the midbrain were separated through an SDS-polyacrylamide gel and transferred onto a membrane. The membrane was probed with either LB509 (upper panel), NACP5 (middle panel) or anti-NSE antibody (lower panel).

### 2.4. Immunohistochemical analysis

The dissected brain was embedded in paraffin and 3 μm-thick serial sections were prepared. To prepare 'mirror sections', the cutting side of two adjacent sections were placed face up on a slide glass. The sections were incubated with LB509 (1:2000 dilution), NACP5 (1:600 dilution) or anti-TH antibody (1:400 dilution). Biotin-labeled secondary antibodies (Vector Laboratories, Burlingame, CA) were used at 10 μg/ml. Immunoreactivities were detected with diaminobenzidine, and nuclei were counterstained with hematoxylin. For double immunofluorescence staining, Alexa Fluor 488 goat anti-mouse IgG and Alexa Fluor 568 goat anti-rabbit IgG (Invitrogen, Carlsbad, CA) were used as secondary antibodies at a dilution of 1:1000.

### 2.5. Quantification of DAergic neurons

Three micrometer-thick serial sections were prepared from the midbrain and stained with anti-TH antibody. The sections were observed at low magnification (4× objective), and the SNc and the ventral tegmental area (VTA) regions were individually outlined according to the brain map (Paxinos and Franklin, 2001). The section with the following anatomical landmark was designated as section #2; that is, a section in which the SNc was divided by the medial terminal nucleus of the accessory optic tract (i.e., the coordinate measured from the interaural line was 0.64 mm). The number of TH-positive cells in sections from #1 to #8 (30 μm intervals) was counted at higher magnification (40× objective) by the fractionator procedure using the StereoInvestigator system (MicroBrightfield, Williston, VT).

### 2.6. Real-time PCR analysis

Total RNA (1 μg) extracted from the midbrain or the whole embryonic brain was subjected to reverse transcription in the presence of 0.2 μg of oligo(dT)$_{12-18}$. Real-time quantitative PCR was carried out with SYBR Green PCR Master mix (Applied Biosystems, Foster City, CA). Gene-specific primers used for the analysis were as follows: TH, 5′-ttgaaggaacggactggctt and 5′-gaaacacacggaaggccaga; DA transporter (DAT), 5′-ccgtatctgtgaggcatctgt and 5′-aacgccaagggagaagcac; c-ret, 5′-tagccactgaccggcagac and 5′-aatggatgtcccctccacag; glutamic acid decarboxylase 1 (GAD1), 5′-agcatcatggctgctcgttacaag and 5′-attgtcggttccaaagccaagc; glial fibrillary acidic protein (GFAP), 5′-agctcaatgaccgctttgctag and 5′-ctggtagacatcagccagtttg; S26 ribosomal protein (Vincent et al., 1993), 5′-ccccaccacgattcagacc and 5′-acggcctctttacatgggc. A primer set for glyceraldehyde 3-phosphate dehydrogenase (GAPDH) was purchased from Applied Biosystems. The cycle profile consisted of 1 min at 95 °C for denaturation and 1 min at 60 °C for annealing and primer extension. Fluorescence was detected by ABI PRISM 7700 sequence detection systems (Applied Biosystems), and mRNA levels were normalized relative to that of GAPDH.

### 2.7. Measurement of monoamine contents

Brain sections were homogenized in a buffer containing 0.2 M perchloric acid, 100 μM ethylenediaminetetraacetic acid (EDTA) and 10 μM pargyline. After centrifugation, DA, its metabolites [i.e., homovanillic acid (HVA) and 3,4-dihydroxyphenylacetic acid (DOPAC)] and serotonin in the supernatant were separated thorough EICOMPAK SC-5ODS

(150 mm × 3.0 mm, Eicom, Kyoto, Japan) with a mobile phase consisting of 0.1 M citrate–acetate buffer, pH 3.9, 18% methanol, 190 mg/l sodium octanslufonate and 5 mg/l EDTA (column temperature: 30 °C; flow-rate: 0.5 ml/min), and detected with an electrochemical detector (NANOSPACE SI-1/2005, Shiseido, Tokyo, Japan). External standards were similarly separated after each chromatographic run for identification and quantification of the peaks.

### 2.8. Behavioral tests

Male Tg mice and age-matched non-Tg littermates were individually housed into an opaque polypropylene cage with ad libitum access to food and water during 12-h light:12-h dark cycle in a sound-proof room. The mice were allowed to acclimatize to the new environment for 15 h before experiment. Spontaneous locomotor activities were recorded with Absystem apparatus (Neuroscience, Tokyo, Japan). L-DOPA (Sigma, St. Louis, MO) was suspended in saline containing 0.1% ascorbic acid. The suspension, which did not contain a DOPA-decarboxylase inhibitor, was subcutaneously administered at a dose of 150 mg/kg, and spontaneous locomotor activities were recorded for 3 h. The concentration of L-DOPA employed in the present study was within the appropriate range especially when a DOPA-decarboxylase inhibitor was not co-administered (Kaur and Starr, 1995; Sotnikova et al., 2005).

### 2.9. Statistical analysis

The data are presented as mean ± S.E.M. Differences between groups were examined for statistical significance using two-tailed Student's *t*-test (for single comparison), one-way analysis of variance (ANOVA) followed by Dunnett's multiple comparison test or two-way ANOVA when appropriate. A *p*-value less than 0.05 denoted the presence of a statistically significant difference.

## 3. Results

### 3.1. Generation of Tg mice

We generated nine Tg lines that expressed human α-synuclein that carried an A53T point mutation and lacked 10 amino acid residues from the C-terminus (hα-syn130m) under the control of the rat TH promoter (i.e., the 9-kb 5′-flanking region of the rat TH gene; Fig. 1a), which drives tissue-specific expression of a reporter gene in transgenic mice (Min et al., 1994). Two independent high expressing lines were selected and named Syn130m-1702 and Syn130m-2402. FISH analysis showed that the insertion sites of the transgene were 8B3 and 12B3 for lines 1702 and 2402, respectively. As a control, we also generated five Tg lines that expressed full-length human α-synuclein(A53T) (hα-syn140m) under the control of the same promoter (Fig. 1a), and the highest expressing line was named Syn140m. Homozygous Syn140m mice were generated so that the expression level of the transgene was comparable to those of heterozygous Syn130m mice. Thus, heterozygous Syn130m and homozygous Syn140m mice were analyzed hereafter unless otherwise mentioned.

Expression of the transgenes in the brain of Syn130m and Syn140m mice was analyzed, and the results are shown in Fig. 1(b–d). The estimated copy numbers of the transgenes per haploid genome were approximately 30 for Syn130m-1702 and 20 for Syn130m-2402 and Syn140m (Fig. 1b). The results of Northern blot analysis were consistent with the copy numbers (Fig. 1c). Immunoblot analysis with LB509 detected single bands of approximately 17 and 19 kDa, which correspond to hα-syn130m and hα-syn140m, respectively (Fig. 1d; upper panel). NACP5 reacted with hα-syn140m as well as mouse α-synuclein migrated at the same position in the gel for Syn140m mice, while the antibody detected two discrete bands corresponding to hα-syn130m (lower band) and mouse α-synuclein (upper band) for Syn130m mice (Fig. 1d; middle panel).

Quantitative immunoblot analysis of the transgene products in the midbrain indicated that the total amounts of α-synuclein (i.e., the transgene product + mouse α-synuclein) in the midbrain of Syn140m, Syn130m-1702 and Syn130m-2402 were 56.8 ± 1.5, 50.5 ± 1.8 and 45.7 ± 1.1 ng per 100 μg of cytoplasmic protein, which were 1.62, 1.44 and 1.31 times, respectively, more abundant than those in age-matched non-Tg littermates. The expression levels of the transgenes in the midbrain did not change significantly by aging; i.e., 103.1 ± 9.3 and 86.8 ± 3.8% at 52 weeks of age compared with 8 weeks of age for Syn140m and Syn130m-1702, respectively. These data indicate that the rat TH promoter is almost constitutively active in the midbrain for at least 52 weeks.

### 3.2. Immunohistochemical analysis of the brain of Tg mice

We carried out immunostaining of coronal sections through the midbrain of Tg mice with LB509 and an anti-TH antibody. Since basically similar results were obtained with both of the Syn130m lines, representative data for line 1702 are shown. LB509 detected the transgene products in the soma and axons of neurons in the SNc [closed arrowheads in Fig. 2a (Syn130m) and b (Syn140m)] and the VTA [open arrowheads in Fig. 2a (Syn130m) and b (Syn140m)]. On the other hand, no immunoreactivity was observed in the corresponding areas of age-matched non-Tg littermates (Fig. 2c). Examination of 'mirror sections' prepared from the midbrain of Tg mice indicated that the transgene products were localized not only in the cytoplasm, but also in the nuclei (Fig. 2d; closed arrowhead), while TH was localized only in the cytoplasm (Fig. 2e; closed arrowhead). The transgene products were transported to presynaptic termini in the striatum (Fig. 2f) and the nucleus accumbens (data

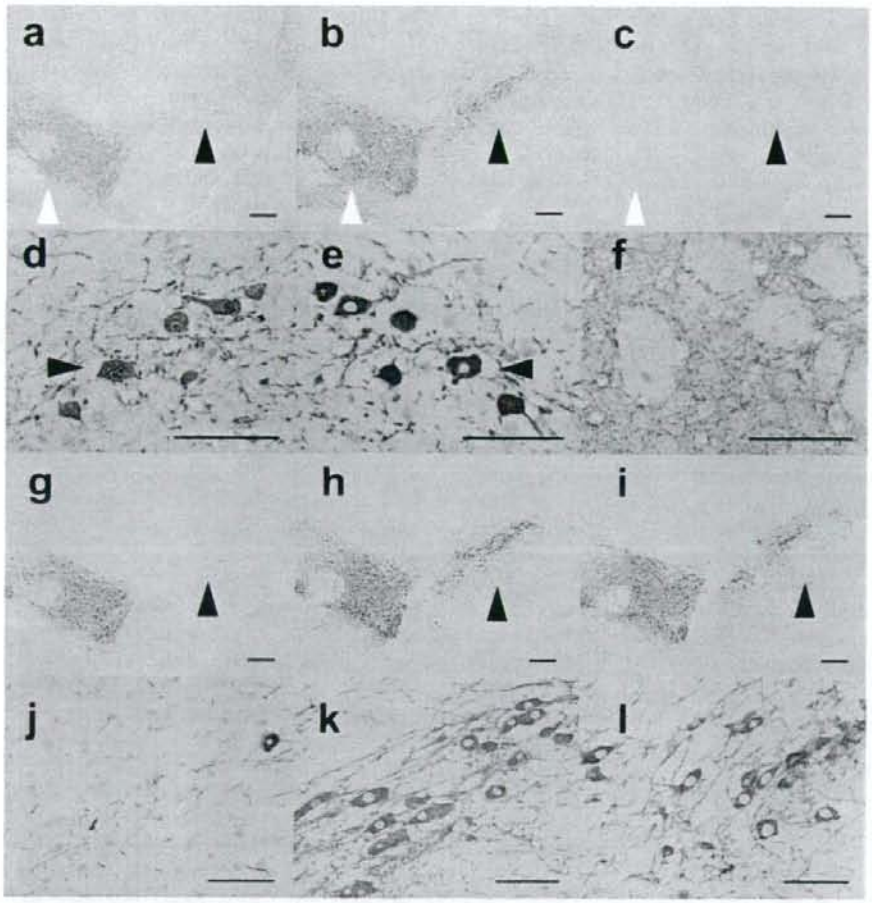


Fig. 2. Immunohistochemical analysis of the brain of Tg mice. (a–c) Coronal sections prepared from the midbrain of Syn130m-1702 (a), Syn140m (b) and an age-matched non-Tg littermate (c), were stained with LB509. Open and closed arrowheads indicate the VTA and SNc, respectively. (d and e) Mirror sections prepared from the SNc region of Syn140m mice were stained with either LB509 (d) or anti-TH antibody (e). Closed arrowheads indicate the same neuron. (f) A section prepared from the striatum of Syn140m mice was stained with LB509. Coordinate measured from the interaural line was 4.8 mm. (g–l) The midbrain of Syn130m-1702 (g and j), Syn140m mice (h and k) and age-matched non-Tg littermates (i and l) were stained with anti-TH antibody. The midbrain was observed at lower magnification (g–i), and the SNc region was observed at higher magnification (j–l). Closed arrowheads in g–i indicate the SNc. Scale bar: 50 μm (a–c and g–i) or 200 μm (d–f and j–l).

not shown), which receive projections from the SNc and the VTA, respectively. The expression profiles of the transgenes were indistinguishable to each other between Syn140m and Syn130m mice, indicating that the C-terminal truncation by at least 10 amino acid residues did not affect the localization of human α-synuclein.

Notably, LB509-immunoreacitvity in the SNc of Syn130m mice (Fig. 2a; closed arrowhead) was weaker than that of Syn140m mice (Fig. 2b; closed arrowhead). Moreover, the TH-immunoreactivity was reduced in the SNc of Syn130m mice (Fig. 2g; closed arrowhead) compared with Syn140m mice (Fig. 2h; closed arrowhead) or non-Tg littermates (Fig. 2i; closed arrowhead). Examination of this region at higher magnification demonstrated this reduction more clearly [Fig. 2j (Syn130m) versus k (Syn140m) and l (non-Tg littermates)]. These data raised the possibility that DAergic neurons were diminished in the SNc of Syn130m mice. In order to test this hypothesis, we carried out a series of experiments. First, locations of TH-positive neurons in sections prepared from the midbrain were spotted on the brain map. This analysis clearly demonstrated a decrease in the number of TH-positive neurons in the SNc of Syn130m mice (Fig. 3a; closed circles) compared with non-Tg littermates (Fig. 3b; closed circles). In particular, the TH-positive neurons were markedly diminished in the lateral part of the SNc in Syn130m mice (Fig. 3a; top and middle arrowheads). On the other hand, the nigral TH-positive neurons clustered on the border of the VTA seemed to be

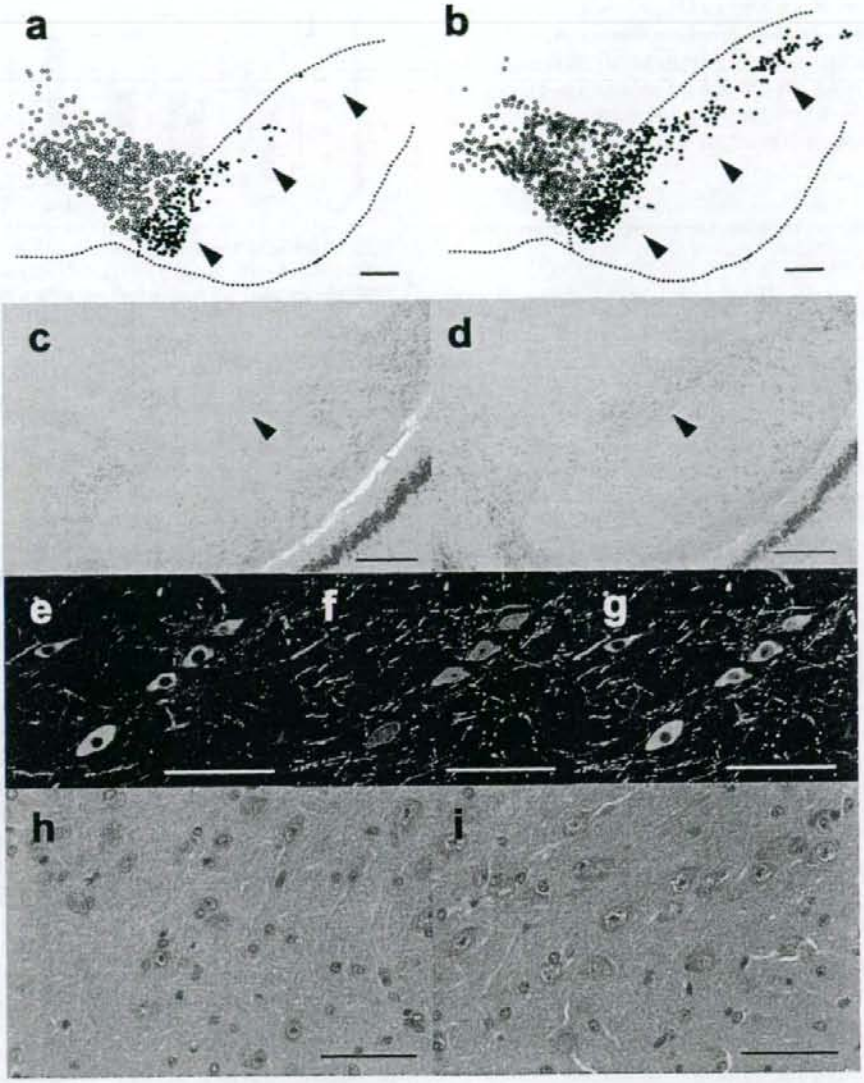


Fig. 3. Neuropathology in the SNc of Syn130m mice. (a and b) Serial sections prepared from the midbrain were stained with anti-TH antibody, and eight sections were selected as described in Materials and methods. The locations of TH-positive neurons in sections #1 to #4 for Syn130m-1702 (a) and an age-matched non-Tg littermate (b) are spotted on the brain map. DAergic neurons in the SNc and the VTA are indicated by closed and open circles, respectively. (c and d) Nissl staining was applied to coronal sections (50 μm-thick) through the midbrain of Syn130m-1702 (c) and an age-matched non-Tg littermate (d). Closed arrowheads indicate the SNc region. (e–g) A coronal section through the midbrain of Syn130m-1702 was stained with anti-TH antibody + Alexa Fluor 568 goat anti-rabbit IgG (e) and LB509 + Alexa Fluor 488 goat anti-mouse IgG (f). Images for TH (red; e) and human α-synuclein (green; f) were merged (g). (h and i) H&E staining was applied to coronal sections through the SNc region of Syn130m-1702 (h) and an age-matched non-Tg littermate (i). Scale bar 200 μm (a–d) or 50 μm (e–i).

less affected (Fig. 3a; bottom arrowhead) than those in the lateral part. In marked contrast to the SNc, TH-positive neurons in the VTA were relatively spared even in Syn130m mice [Fig. 3a (Syn130m) versus b (non-Tg littermates); open circles]. Furthermore, Nissl staining revealed considerable loss of neuronal cell bodies in the SNc region of Syn130m mice (Fig. 3c; closed arrowhead) compared with the control mice (Fig. 3d; closed arrowhead). Third, a section through the SNc region of Syn130m mice was subjected to double immunofluorescence staining with LB509 and anti-TH antibody. Merged images of TH (Fig. 3e) and LB509 (Fig. 3f) showed that most of the LB509-positive cells were concomitantly TH-positive (Fig. 3g), though reduced expression of TH in LB509-positive neurons would have resulted in

robust increase in LB509 (+)/TH (−) cells. Finally, H&E staining showed the loss of neurons in the SNc [Fig. 3h (Syn130m) versus i (non-Tg littermates)]. Taken together, these data strongly suggest that the reduction in TH-positive cells in the SNc of Syn130m mice was primarily due to actual loss of DAergic neurons rather than reduced expression of TH.

### 3.3. Quantification of the loss of nigral DAergic neurons in the Tg mice

Quantification of mesencephalic DAergic neurons in Syn130m mice revealed that approximately 45 and 19% of DAergic neurons were significantly lost in the SNc of Syn130m-1702 (Fig. 4a, SNc; closed bar) and Syn130m-2402 (Fig. 4a, SNc; hatched bar), respectively, compared with non-Tg littermates (Fig. 4a, SNc; open bar) at 8 weeks of age. On the other hand, no apparent loss of nigral DAergic neurons was noted in Syn140m mice at the same age (Fig. 4a, SNc; gray bar). In contrast to the SNc, no such loss was observed in the VTA of Syn130m (Fig. 4a, VTA; closed and hatched bars) and Syn140m mice (Fig. 4a, VTA; gray bar) compared with non-Tg littermates (Fig. 4a, VTA; open bar), indicating a selective neuronal loss in the SNc of Syn130m mice. Interestingly, the loss of nigral DAergic neurons in Syn130m mice was not progressive and was stable

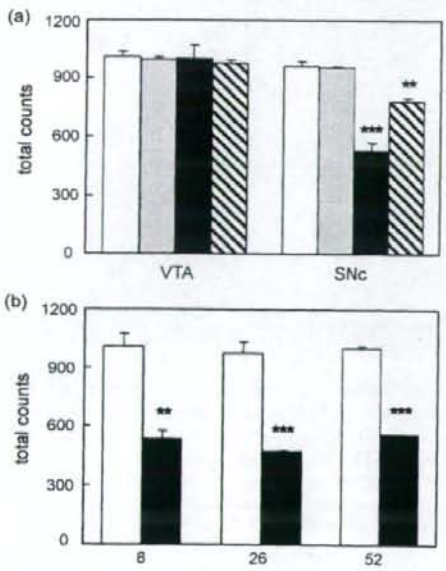


Fig. 4. Quantification of mesencephalic DAergic neurons. The number of TH-positive neurons in the designated area of the midbrain was quantified as described in Section 2.5. (a) The numbers of TH-positive neurons in the VTA and the SNc are individually shown for non-Tg littermates (open bars), Syn140m mice (gray bars), Syn130m-1702 (closed bars) and Syn130m-2402 (hatched bars). (b) The numbers of TH-positive neurons in the SNc of Syn130m-1702 (closed bars) and non-Tg littermates (open bars) were quantified at 8, 26 and 52 weeks of age. $^{**}p<0.01$; $^{***}p<0.001$ ($n=3$).

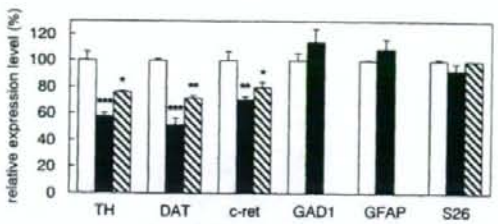


Fig. 5. Real-time PCR analysis of the loss of DAergic neurons. Total RNAs were extracted from the midbrain of Syn130m-1702 (closed bars), Syn130m-2402 (hatched bars) and non-Tg littermates (open bars). The expression levels of TH, DAT, c-ret, GAD1, GFAP and S26 were quantified by real-time PCR analysis. The data were normalized to that for GAPDH. $^{*}p<0.05$; $^{**}p<0.01$; $^{***}p<0.001$ ($n=3$).

up to 52 weeks of age (Fig. 4b). These findings were confirmed by several other methods. Quantitative immunoblot analysis showed that the relative densities of TH in the midbrain of Syn130m-1702 and Syn130m-2402 decreased to $60.2 \pm 3.3$ and $71.3 \pm 3.8\%$, respectively, relative to those of age-matched non-Tg littermates, while no significant decrease was observed in Syn140m mice. Furthermore, real-time PCR analysis indicated that the expression levels of TH, DAT and c-ret, which are specifically expressed in DAergic neurons, were significantly diminished in the midbrain of Syn130m-1702 (Fig. 5; closed bars) and Syn130m-2402 (Fig. 5; hatched bars) compared with age-matched non-Tg littermates (Fig. 5; open bars). On the other hand, expressions of GAD1 and GFAP, which are predominantly expressed in GABAergic neurons and astrocytes, respectively, were not affected at all in Syn130m mice (Fig. 5). Collectively, these data support the notion that a proportion of DAergic neurons are lost in the SNc of Syn130m mice.

### 3.4. Behavioral abnormalities of the Tg mice

The data in Figs. 4 and 5 indicate that the loss of nigral DAergic neurons in Syn130m mice was severe in line 1702 than in line 2402. Therefore, the former line was extensively analyzed hereafter. In accordance with the selective loss of nigral DAergic neurons, TH-positive neurites were markedly impaired in the striatum of Syn130m mice (Fig. 6a). On the other hand, no overt abnormalities were observed in the nucleus accumbens which receive projections from the VTA (data not shown). As a result, striatal TH was decreased to $38.1 \pm 3.2\%$ of the control at 8 weeks of age (Fig. 6b; TH). Consequently, striatal contents of DA and HVA, one of the major metabolites of DA, were significantly reduced to $48.8 \pm 2.2$ and $51.9 \pm 1.6\%$, respectively, relative to those of non-Tg littermates of the same age (Fig. 6b; DA and HVA). The amount of DOPAC, another metabolite of DA, in the striatum was also decreased to a similar extent (data not shown). On the other hand, there was no significant difference in the serotonin content between Syn130m mice and non-Tg littermates (Fig. 6b; serotonin). The amounts of TH and DA in the striatum did not show an age-dependent decrease but

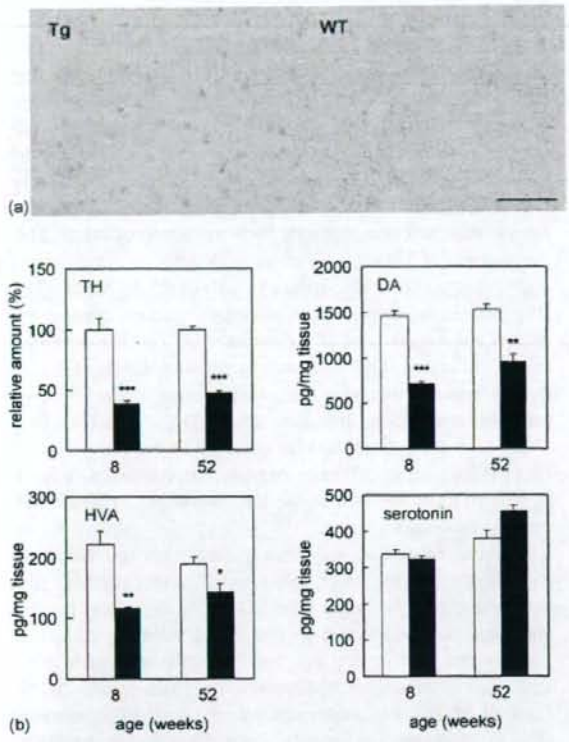


Fig. 6. Neuropathology in the striatum. (a) Coronal sections of the midbrain of Syn130m-1702 (Tg) and an age-matched non-Tg littermate (WT) were stained with anti-TH antibody. Coordinate measured from the interaural line was 2.9 mm. Scale bar: 200 μm. (b) The amounts of TH, DA, HVA and serotonin in the striatum of Syn130m-1702 (closed bars) and age-matched non-Tg littermates (open bars) were measured at 8 and 52 weeks of age. $^{*}p<0.05$; $^{**}p<0.01$; $^{***}p<0.001$ ($n=4$).

plateaued to a similar extent up to 52 weeks of age (Fig. 6b; TH and DA).

The striatal impairments in Syn130m mice prompted us to conduct a battery of motor function tests (e.g. rotarod test, pole test, traction test and catalepsy test). However, no motor deficits were detected by these tests. Notably, both diurnal and nocturnal spontaneous locomotor activities of Syn130m mice were markedly reduced compared with the control (Fig. 7a), though the rectal temperature was not significantly different. It is known that the loss of striatal dopamine causes behavioral deficits, which improve with L-DOPA, the precursor of DA and the most commonly used drug for PD (Tillerson et al., 2002). Therefore, we examined the effect of L-DOPA on the behavioral abnormalities of Syn130m mice. The Tg mice showed significant recovery in locomotor activity following a single subcutaneous injection of L-DOPA (150 mg/kg), whereas the drug at this concentration did not affect the behavior of non-Tg littermates (Fig. 7b). These data suggest that the decrease in the spontaneous locomotor activities of Syn130m mice was related to the striatal DA content.

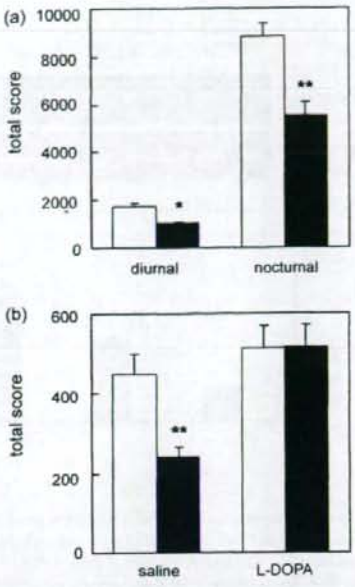


Fig. 7. Effect of L-DOPA on the behavioral abnormalities of Tg mice. (a) Spontaneous locomotor activities of Syn130m-1702 (closed bars) and age-matched non-Tg littermates (open bars) in the light (diurnal) and dark (nocturnal) periods are individually shown. (b) Suspension of L-DOPA (150 mg/kg) was injected subcutaneously in Syn130m-1702 (closed bars) and age-matched non-Tg littermates (open bars) during light period. Spontaneous locomotor activities were measured for 3 h (from 0.5 to 3.5 h after administration). $^{*}p<0.05$; $^{**}p<0.01$ [$n=11$ (a); $n=17$ (b)].

### 3.5. Loss of nigral DAergic neurons during embryogenesis

In an attempt to elucidate the mechanism of the selective neuronal loss in Syn130m mice, we tried to generate homozygotes of line 1702 expecting much severer phenotype. Genotyping of the embryos revealed that intercross of heterozygotes produced offspring of all three different genotypes according to Mendel's laws, indicating that homozygotes are not embryonic lethal. However, none of the weaned pups was homozygous. We then delivered the offspring by Caesarean section on days 19 post-coitus, and found that homozygotes had relatively higher incidence of apneas after delivery (10/16) compared with heterozygotes (6/28) and non-Tg littermates (2/14). In addition, none of the homozygous neonates survived beyond postnatal day 1. Genotyping and quantitative immunoblot analysis of the neonates indicated that the expression level of hα-syn130m was almost proportional to the gene dosage, while the relative amount of TH was markedly decreased in inverse proportion to the gene dosage (supplemental data). Taken together, these results unequivocally indicate that the loss of DAergic neurons correlate strongly with the expression level of hα-syn130m.

The data described above suggest that the neuronal loss takes place during embryogenesis. To address this issue, we

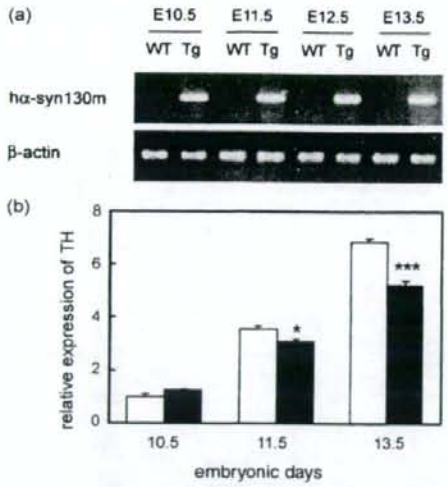


Fig. 8. Analysis of embryonic brain. Total RNAs were extracted from the whole embryonic brain of Syn130m-1702 [Tg (a) and closed bars (b)] and non-Tg littermates [WT (a) and open bars (b)] at E10.5, E11.5, E12.5 and E13.5. (a) Expression of the transgene was analyzed by RT-PCR. (b) Expression of TH was quantified by real-time PCR analysis. The data were normalized to that for GAPDH. $^{*}p<0.05$; $^{***}p<0.001$ ($n=4$–6).

analyzed the embryonic brain prepared at various stages of gestation. RT-PCR analysis revealed that the transgene was turned on even at 10.5 days of gestation (E10.5; Fig. 8a). Notably, the expression level of TH was significantly lower in Syn130m mice after E11.5 than in non-Tg littermates (Fig. 8b). However, the number of TUNEL-positive and anti-activated caspase 3 antibody-positive cells in the embryonic brain of Syn130m mice were not significantly different from the control (data not shown). These data strongly suggest that overexpression of hα-syn130m is deleterious to development and/or survival of nigral DAergic neurons during embryogenesis.

## 4. Discussion

Several groups had already generated Tg mice that express full-length α-synuclein under the control of various promoters (Giasson et al., 2002; Kahle et al., 2000; Lee et al., 2002; Masliah et al., 2000; Matsuoka et al., 2001; Neumann et al., 2002; Richfield et al., 2002; van der Putten et al., 2000). In the present study, we generated Tg mice (Syn130m mice) that express C-terminally truncated human α-synuclein (hα-syn130m) under the control of the rat TH promoter so that the transgene is expressed in mesencephalic DAergic neurons (Fig. 2a). Remarkably, nigral TH-positive neurons (A9 cells) were selectively and constitutively reduced in substantial numbers in Syn130m mice (Figs. 2–4). In marked contrast to A9 cells, DAergic neurons in the VTA (A10 cells) were relatively spared (Figs. 3a and 4a). We concluded that this reduction was due to actual loss of A9 cells rather than reduced expression of TH in these cells based on the data of Nissl-staining (Fig. 3c and d), double immunofluorescence staining (Fig. 3e–g), H&E staining (Fig. 3h and i) and real-time PCR analysis (Fig. 5). Though hα-syn130m was also expressed in catecholamine producing cells in several other tissues, such as olfactory bulb, the locus ceruleus and the adrenal medulla, no overt loss of the cells was observed in these loci (data not shown). Therefore, the loss of DAergic neurons seemed to occur specifically in the SNc. The loss of A9 cells was accompanied by a reduction of nigral TH, impairment of TH-positive neurites in the striatum (Fig. 6a) and subsequent decrease in the amounts of striatal TH and DA (Fig. 6b). Examination of the behavioral parameters demonstrated the impairment of spontaneous locomotor activities (Fig. 7a). Since L-DOPA treatment significantly ameliorated the locomotor deficit (Fig. 7b), we postulate that this behavioral abnormality was due to low striatal DA content (Fig. 6b). Other motor functions thus far examined were not impaired in Syn130m mice, probably because the residual DA level in the striatum was still above the threshold to cause other motor dysfunctions.

We carefully and extensively analyzed the brain of Syn130m mice for other pathological abnormalities, and obtained the following results: (1) H&E staining (Fig. 3h) and immunostaining with an anti-GFAP antibody (data not shown) did not detect any sign of gliosis, which generally accompanies neurodegeneration (Vila et al., 2001). Lack of gliosis was confirmed by real-time PCR analysis (Fig. 5). Moreover, immunostaining against Iba1 showed lack of microgliosis (data not shown). These results imply that inflammatory process was not involved in the neuronal loss in Syn130m mice. Given that hα-syn130m is deleterious to the development and/or survival of A9 cells (see below), lack of gliosis is not surprising. (2) It is known that α-synuclein is phosphorylated mainly at Ser129 in LBs (Fujiwara et al., 2002) suggesting that the modification is involved in the pathogenesis of PD (Chen and Feany, 2005). However, DAergic neurons were only faintly immunoreactive to an antibody which specifically reacts to α-synuclein phosphorylated at Ser129 (data not shown) (Fujiwara et al., 2002). This is probably because hα-syn130m lacks a part of the consensus recognition sequence for casein kinases or G-protein coupled receptor kinases, which were reported to be responsible for the phosphorylation at Ser129 (Okochi et al., 2000; Pronin et al., 2000). Therefore, Ser129 might not have been phosphorylated effectively. (3) It has been reported that C-terminally truncated α-synuclein forms aggregates much faster than the full-length protein in vitro (Crowther et al., 1998; Du et al., 2003; Murray et al., 2003). Though this is also the case with hα-syn130m (Yoshimoto et al., unpublished observations), LB-like structures were not detected in the brain of Syn130m mice by H&E staining (Fig. 3h) or immunostaining with anti-ubiquitin antibodies (data not shown). Moreover, in our hand immunoblot analysis did not detect aggregated α-synuclein in the brain (data not shown). Collectively, it seems that neuronal loss in Syn130m mice took place in the absence of LB formation. These data may be consistent with the finding

that α-synuclein inclusion bodies are not toxic to the neurons (Chen and Feany, 2005).

The data of the present study strongly suggest that overexpression of hα-syn130m is deleterious to normal development and/or survival of A9 cells during embryogenesis (Fig. 8b). The mechanism of the selective toxicity of hα-syn130m remains unclear. The possibility that the phenotype of Syn130m mice was caused by insertional mutagenesis was excluded since the integration sites of the transgene were different from each other for two independent Tg lines which showed similar phenotype (8B3 and 12B3 for lines 1702 and 2402, respectively). It seems that the expression level of the transgene per se is an important factor for the neuronal loss, because loss of A9 cells seemed to be dependent on the expression level of hα-syn130m (Figs. 4a and 5 and supplemental data). In addition, other Tg lines that expressed hα-syn130m at lower level did not develop similar phenotype. Nevertheless, it is likely that truncation of human α-synuclein(A53T) is primarily responsible for the selective loss of A9 cells since homozygous Syn140m mice, in which comparable amount of hα-syn140m was expressed in the midbrain, did not develop such a phenotype at 8 weeks (Figs. 2h and k and 4a) or even at 18 months of age (data not shown). Therefore, it may be conceivable that truncated human α-synuclein gains toxic functions and exerts deleterious effects to A9 cells in a dominant fashion, though the possibility that the truncated protein fails to protect A9 progenitor cells from various insults such as oxidative damage (Albani et al., 2004; Kanda et al., 2000; Liu et al., 2005) cannot be completely ruled out.

Our data suggest that a truncation by only 10 amino acid residues from the C-terminus would be sufficient to produce toxic effects on A9 cells, though several C-terminally truncated species of α-synuclein accumulate in the brain of PD patients (Campbell et al., 2001; Li et al., 2005; Liu et al., 2005; Tofaris et al., 2003). It may be noteworthy that not only A10 cells but also A9 cells clustering on the border of the VTA seem to be relatively less susceptible to the "toxicity" of hα-syn130m (Fig. 3a). These data, together with the fact that the loss of A9 cells was not progressive (Fig. 4b), imply the existence of subpopulations of DAergic neurons within A9 cell groups in terms of susceptibility to hα-syn130m.

Recently, Tofaris et al. (2006) reported a Tg line that express C-terminally truncated human α-synuclein (amino acid residue number: 1–120) under the control of the TH promoter. The major difference between their Tg mice and Syn130m mice is that the former express wild type human α-synuclein(1–120) and lack endogenous α-synuclein, while the latter express both mutant human α-synuclein(1-130) and intact endogenous α-synuclein. Despite the difference in the genetic background and the length of the truncation, striatal DA level was almost constitutively reduced in both of the Tg lines. Therefore, our results complement the notion that C-terminally truncated α-synuclein affects the development of DAergic system. The other reported phenotypes were not observed in our Tg mice (i.e., pathological inclusions and microgliosis). It is currently unclear if these differences are solely derived from the difference in the length of the truncation.

In conclusion, we generated Tg mice that recapitulate some of typical features of PD (i.e., selective loss of nigral DAergic neurons, subsequent decrease in striatal DA content and behavioral abnormalities that can be rectified with L-DOPA). Since DAergic neurons are affected during embryogenesis and the neuronal loss does not progress after birth, these Tg mice have limitations to use as an animal model of PD. However, these Tg mice are useful to investigate the toxicity of α-synuclein to nigral DAergic neurons in vivo. In addition, the early onset of the symptoms is advantageous to explore therapeutic possibilities for PD.

## Conflict of interest

Masaki Wakamatsu, Aiko Ishii, Shingo Iwata, Junko Sakagami, Yuriko Ukai, Mieko Ono, Daiji Kanbe and Makoto Yoshimoto are the employees of Taisho Pharmaceutical Co., Ltd. Shin-ichi Muramatsu has no conflicts of interest.

## Disclosure

The data in this manuscript have not been previously published, have not been submitted elsewhere and will not be submitted elsewhere while under consideration at Neurobiology of Aging. All the animal experiments reported in this manuscript were carried out in accordance with guidelines of the Japanese Association for Laboratory Animal Science. All authors have reviewed the contents of this manuscript and validated the accuracy of the data.

## Acknowledgments

We thank Drs. Hitoshi Takahashi and Akiyoshi Kakita at Brain Disease Research Center, Niigata University for their helpful suggestions during the preparation of this manuscript. We are also grateful to Ms. Keiko Chiba for the technical assistance in the preparation of the transgene constructs. This study was financially supported by Taisho Pharmaceutical Co., Ltd.

## Appendix A. Supplementary data

Supplementary data associated with this article can be found, in the online version, at doi:10.1016/j.neurobiolaging.2006.11.017.

## References

Albani, D., Peverelli, E., Rametta, R., Batelli, S., Veschini, L., Negro, A., Forloni, G., 2004. Protective effect of TAT-delivered alpha-synuclein:

relevance of the C-terminal domain and involvement of HSP70. Faseb J. 18, 1713–1715.

Arawaka, S., Saito, Y., Murayama, S., Mori, H., 1998. Lewy body in neurodegeneration with brain iron accumulation type 1 is immunoreactive for alpha-synuclein. Neurology 51 (3), 887–889.

Arima, K., Ueda, K., Sunohara, N., Hirai, S., Izumiyama, Y., Tonozuka-Uehara, H., Kawai, M., 1998. Immunoelectron-microscopic demonstration of NACP/alpha-synuclein-epitopes on the filamentous component of Lewy bodies in Parkinson's disease and in dementia with Lewy bodies. Brain Res. 808 (1), 93–100.

Baba, M., Nakajo, S., Tu, P.H., Tomita, T., Nakaya, K., Lee, V.M., Trojanowski, J.Q., Iwatsubo, T., 1998. Aggregation of alpha-synuclein in Lewy bodies of sporadic Parkinson's disease and dementia with Lewy bodies. Am. J. Pathol. 152 (4), 879–884.

Campbell, B.C., McLean, C.A., Culvenor, J.G., Gai, W.P., Blumbergs, P.C., Jakala, P., Beyreuther, K., Masters, C.L., Li, Q.X., 2001. The solubility of alpha-synuclein in multiple system atrophy differs from that of dementia with Lewy bodies and Parkinson's disease. J. Neurochem. 76 (1), 87–96.

Chen, L., Feany, M.B., 2005. Alpha-synuclein phosphorylation controls neurotoxicity and inclusion formation in a Drosophila model of Parkinson disease. Nat. Neurosci. 8 (5), 657–663.

Crowther, R.A., Jakes, R., Spillantini, M.G., Goedert, M., 1998. Synthetic filaments assembled from C-terminally truncated alpha-synuclein. FEBS Lett. 436 (3), 309–312.

Du, H.N., Tang, L., Luo, X.Y., Li, H.T., Hu, J., Zhou, J.W., Hu, H.Y., 2003. A peptide motif consisting of glycine, alanine, and valine is required for the fibrillization and cytotoxicity of human alpha-synuclein. Biochemistry 42 (29), 8870–8878.

Fujiwara, H., Hasegawa, M., Dohmae, N., Kawashima, A., Masliah, E., Goldberg, M.S., Shen, J., Takio, K., Iwatsubo, T., 2002. alpha-Synuclein is phosphorylated in synucleinopathy lesions. Nat. Cell. Biol. 4 (2), 160–164.

Giasson, B.I., Duda, J.E., Quinn, S.M., Zhang, B., Trojanowski, J.Q., Lee, V.M., 2002. Neuronal alpha-synucleinopathy with severe movement disorder in mice expressing A53T human alpha-synuclein. Neuron 34 (4), 521–533.

Hogan, B., Beddington, R., Costantini, F., Lacy, E., 1994. Manipulating the Mouse Embryo, Second ed. Cold Spring Harbor Laboratory Press, Plainview.

Iwai, A., Masliah, E., Yoshimoto, M., Ge, N., Flanagan, L., de Silva, H.A., Kittel, A., Saitoh, T., 1995. The precursor protein of non-A beta component of Alzheimer's disease amyloid is a presynaptic protein of the central nervous system. Neuron 14 (2), 467–475.

Iwawaki, T., Kohno, K., Kobayashi, K., 2000. Identification of a potential nurr1 response element that activates the tyrosine hydroxylase gene promoter in cultured cells. Biochem. Biophys. Res. Commun. 274 (3), 590–595.

Jakes, R., Crowther, R.A., Lee, V.M., Trojanowski, J.Q., Iwatsubo, T., Goedert, M., 1999. Epitope mapping of LB509, a monoclonal antibody directed against human alpha-synuclein. Neurosci. Lett. 269 (1), 13–16.

Kahle, P.J., Neumann, M., Ozmen, L., Muller, V., Jacobsen, H., Schindzielorz, A., Okochi, M., Leimer, U., van Der Putten, H., Probst, A., Kremmer, E., Kretzschmar, H.A., Haass, C., 2000. Subcellular localization of wild-type and Parkinson's disease-associated mutant alpha-synuclein in human and transgenic mouse brain. J. Neurosci. 20 (17), 6365–6373.

Kanda, S., Bishop, J.F., Eglitis, M.A., Yang, Y., Mouradian, M.M., 2000. Enhanced vulnerability to oxidative stress by alpha-synuclein mutations and C-terminal truncation. Neuroscience 97 (2), 279–284.

Kaur, S., Starr, M.S., 1995. Antiparkinsonian action of dextromethorphan in the reserpine-treated mouse. Eur. J. Pharmacol. 280 (2), 159–166.

Kobayashi, K., Sasaoka, T., Morita, S., Nagatsu, I., Iguchi, A., Kurosawa, Y., Fujita, K., Nomura, T., Kimura, M., Katsuki, M., Nagatsu, T., 1992. Genetic alteration of catecholamine specificity in transgenic mice. Proc. Natl. Acad. Sci. U.S.A. 89 (5), 1631–1635.

Kruger, R., Kuhn, W., Muller, T., Woitalla, D., Graeber, M., Kosel, S., Przuntek, H., Epplen, J.T., Schols, L., Riess, O., 1998. Ala30Pro mutation in the gene encoding alpha-synuclein in Parkinson's disease. Nat. Genet. 18 (2), 106–108.

Lee, M.K., Stirling, W., Xu, Y., Xu, X., Qui, D., Mandir, A.S., Dawson, T.M., Copeland, N.G., Jenkins, N.A., Price, D.L., 2002. Human alpha-synuclein-harboring familial Parkinson's disease-linked Ala-53 → Thr mutation causes neurodegenerative disease with alpha-synuclein aggregation in transgenic mice. Proc. Natl. Acad. Sci. U.S.A. 99 (13), 8968–8973.

Li, W., West, N., Colla, E., Pletnikova, O., Troncoso, J.C., Marsh, L., Dawson, T.M., Jakala, P., Hartmann, T., Price, D.L., Lee, M.K., 2005. Aggregation promoting C-terminal truncation of alpha-synuclein is a normal cellular process and is enhanced by the familial Parkinson's disease-linked mutations. Proc. Natl. Acad. Sci. U.S.A. 102 (6), 2162–2167.

Liu, C.W., Giasson, B.I., Lewis, K.A., Lee, V.M., Demartino, G.N., Thomas, P.J., 2005. A precipitating role for truncated alpha-synuclein and the proteasome in alpha-synuclein aggregation: implications for pathogenesis of Parkinson disease. J. Biol. Chem. 280 (24), 22670–22678.

Masliah, E., Rockenstein, E., Veinbergs, I., Mallory, M., Hashimoto, M., Takeda, A., Sagara, Y., Sisk, A., Mucke, L., 2000. Dopaminergic loss and inclusion body formation in alpha-synuclein mice: implications for neurodegenerative disorders. Science 287 (5456), 1265–1269.

Matsuoka, Y., Vila, M., Lincoln, S., McCormack, A., Picciano, M., LaFrancois, J., Yu, X., Dickson, D., Langston, W.J., McGowan, E., Farrer, M., Hardy, J., Duff, K., Przedborski, S., Di Monte, D.A., 2001. Lack of nigral pathology in transgenic mice expressing human alpha-synuclein driven by the tyrosine hydroxylase promoter. Neurobiol. Dis. 8 (3), 535–539.

Min, N., Joh, T.H., Kim, K.S., Peng, C., Son, J.H., 1994. 5′ upstream DNA sequence of the rat tyrosine hydroxylase gene directs high-level and tissue-specific expression to catecholaminergic neurons in the central nervous system of transgenic mice. Brain Res. Mol. Brain Res. 27 (2), 281–289.

Murray, I.V., Giasson, B.I., Quinn, S.M., Koppaka, V., Axelsen, P.H., Ischiropoulos, H., Trojanowski, J.Q., Lee, V.M., 2003. Role of alpha-synuclein carboxy-terminus on fibril formation in vitro. Biochemistry 42 (28), 8530–8540.

Neumann, M., Kahle, P.J., Giasson, B.I., Ozmen, L., Borroni, E., Spooren, W., Muller, V., Odoy, S., Fujiwara, H., Hasegawa, M., Iwatsubo, T., Trojanowski, J.Q., Kretzschmar, H.A., Haass, C., 2002. Misfolded proteinase K-resistant hyperphosphorylated alpha-synuclein in aged transgenic mice with locomotor deterioration and in human alpha-synucleinopathies. J. Clin. Invest. 110 (10), 1429–1439.

Okochi, M., Walter, J., Koyama, A., Nakajo, S., Baba, M., Iwatsubo, T., Meijer, L., Kahle, P.J., Haass, C., 2000. Constitutive phosphorylation of the Parkinson's disease associated alpha-synuclein. J. Biol. Chem. 275 (1), 390–397.

Paxinos, G., Franklin, K.B.J., 2001. The Mouse Brain in Stereotaxic Coordinates, Second ed. Academic Press, San Diego.

Polymeropoulos, M.H., Lavedan, C., Leroy, E., Ide, S.E., Dehejia, A., Dutra, A., Pike, B., Root, H., Rubenstein, J., Boyer, R., Stenroos, E.S., Chandrasekharappa, S., Athanassiadou, A., Papapetropoulos, T., Johnson, W.G., Lazzarini, A.M., Duvoisin, R.C., Di Iorio, G., Golbe, L.I., Nussbaum, R.L., 1997. Mutation in the alpha-synuclein gene identified in families with Parkinson's disease. Science 276 (5321), 2045–2047.

Pronin, A.N., Morris, A.J., Surguchov, A., Benovic, J.L., 2000. Synucleins are a novel class of substrates for G protein-coupled receptor kinases. J. Biol. Chem. 275 (34), 26515–26522.

Richfield, E.K., Thiruchelvam, M.J., Cory-Slechta, D.A., Wuertzer, C., Gainetdinov, R.R., Caron, M.G., Di Monte, D.A., Federoff, H.J., 2002. Behavioral and neurochemical effects of wild-type and mutated human alpha-synuclein in transgenic mice. Exp. Neurol. 175 (1), 35–48.

Singleton, A.B., Farrer, M., Johnson, J., Singleton, A., Hague, S., Kachergus, J., Hulihan, M., Peuralinna, T., Dutra, A., Nussbaum, R., Lincoln, S., Crawley, A., Hanson, M., Maraganore, D., Adler, C., Cookson, M.R., Muenter, M., Baptista, M., Miller, D., Blancato, J., Hardy, J., Gwinn-Hardy, K., 2003. alpha-Synuclein locus triplication causes Parkinson's disease. Science 302 (5646), 841.

Sotnikova, T.D., Beaulieu, J.M., Barak, L.S., Wetsel, W.C., Caron, M.G., Gainetdinov, R.R., 2005. Dopamine-independent locomotor actions of amphetamines in a novel acute mouse model of Parkinson disease. PLoS Biol. 3 (8), e271.

Spillantini, M.G., Crowther, R.A., Jakes, R., Hasegawa, M., Goedert, M., 1998. Alpha-synuclein in filamentous inclusions of Lewy bodies from Parkinson's disease and dementia with lewy bodies. Proc. Natl. Acad. Sci. U.S.A. 95 (11), 6469–6473.

Takeda, A., Mallory, M., Sundsmo, M., Honer, W., Hansen, L., Masliah, E., 1998. Abnormal accumulation of NACP/alpha-synuclein in neurodegenerative disorders. Am. J. Pathol. 152 (2), 367–372.

Tillerson, J.L., Caudle, W.M., Reveron, M.E., Miller, G.W., 2002. Detection of behavioral impairments correlated to neurochemical deficits in mice treated with moderate doses of 1-methyl-4-phenyl-1,2,3,6-tetrahydropyridine. Exp. Neurol. 178 (1), 80–90.

Tofaris, G.K., Garcia Reitbock, P., Humby, T., Lambourne, S.L., O'Connell, M., Ghetti, B., Gossage, H., Emson, P.C., Wilkinson, L.S., Goedert, M., Spillantini, M.G., 2006. Pathological changes in dopaminergic nerve cells of the substantia nigra and olfactory bulb in mice transgenic for truncated human alpha-synuclein(1–120): implications for Lewy body disorders. J. Neurosci. 26 (15), 3942–3950.

Tofaris, G.K., Razzaq, A., Ghetti, B., Lilley, K.S., Spillantini, M.G., 2003. Ubiquitination of alpha-synuclein in Lewy bodies is a pathological event not associated with impairment of proteasome function. J. Biol. Chem. 278 (45), 44405–44411.

Ueda, K., Fukushima, H., Masliah, E., Xia, Y., Iwai, A., Yoshimoto, M., Otero, D.A., Kondo, J., Ihara, Y., Saitoh, T., 1993. Molecular cloning of cDNA encoding an unrecognized component of amyloid in Alzheimer disease. Proc. Natl. Acad. Sci. U.S.A. 90 (23), 11282–11286.

van der Putten, H., Wiederhold, K.H., Probst, A., Barbieri, S., Mistl, C., Danner, S., Kauffmann, S., Hofele, K., Spooren, W.P., Ruegg, M.A., Lin, S., Caroni, P., Sommer, B., Tolnay, M., Bilbe, G., 2000. Neuropathology in mice expressing human alpha-synuclein. J. Neurosci. 20 (16), 6021–6029.

Vila, M., Jackson-Lewis, V., Guegan, C., Wu, D.C., Teismann, P., Choi, D.K., Tieu, K., Przedborski, S., 2001. The role of glial cells in Parkinson's disease. Curr. Opin. Neurol. 14 (4), 483–489.

Vincent, S., Marty, L., Fort, P., 1993. S26 ribosomal protein RNA: an invariant control for gene regulation experiments in eucaryotic cells and tissues. Nucleic Acids Res. 21 (6), 1498.

Wakabayashi, K., Hayashi, S., Yoshimoto, M., Kudo, H., Takahashi, H., 2000. NACP/alpha-synuclein-positive filamentous inclusions in astrocytes and oligodendrocytes of Parkinson's disease brains. Acta Neuropathol. (Berl.) 99 (1), 14–20.

Wakabayashi, K., Matsumoto, K., Takayama, K., Yoshimoto, M., Takahashi, H., 1997. NACP, a presynaptic protein, immunoreactivity in Lewy bodies in Parkinson's disease. Neurosci. Lett. 239 (1), 45–48.

Zarranz, J.J., Alegre, J., Gomez-Esteban, J.C., Lezcano, E., Ros, R., Ampuero, I., Vidal, L., Hoenicka, J., Rodriguez, O., Atares, B., Llorens, V., Gomez Tortosa, E., del Ser, T., Munoz, D.G., de Yebenes, J.G., 2004. The new mutation, E46K, of alpha-synuclein causes Parkinson and Lewy body dementia. Ann. Neurol. 55 (2), 164–173.

OPEN ACCESS Freely available online

PLoS one

# Ablation of NMDA Receptors Enhances the Excitability of Hippocampal CA3 Neurons

**Fumiaki Fukushima[1], Kazuhito Nakao[1], Toru Shinoe[2¤a], Masahiro Fukaya[3], Shin-ichi Muramatsu[4], Kenji Sakimura[5], Hirotaka Kataoka[1], Hisashi Mori[1¤b], Masahiko Watanabe[3], Toshiya Manabe[2,6], Masayoshi Mishina[1]***

**1** Department of Molecular Neurobiology and Pharmacology, Graduate School of Medicine, University of Tokyo, Tokyo, Japan, **2** Division of Neuronal Network, Institute of Medical Science, University of Tokyo, Tokyo, Japan, **3** Department of Anatomy, Hokkaido University School of Medicine, Sapporo, Japan, **4** Division of Neurology, Department of Medicine, Jichi Medical University, Tochigi, Japan, **5** Department of Cellular Neurobiology, Brain Research Institute, Niigata University, Niigata, Japan, **6** CREST, JST, Kawaguchi, Japan

## Abstract

Synchronized discharges in the hippocampal CA3 recurrent network are supposed to underlie network oscillations, memory formation and seizure generation. In the hippocampal CA3 network, NMDA receptors are abundant at the recurrent synapses but scarce at the mossy fiber synapses. We generated mutant mice in which NMDA receptors were abolished in hippocampal CA3 pyramidal neurons by postnatal day 14. The histological and cytological organizations of the hippocampal CA3 region were indistinguishable between control and mutant mice. We found that mutant mice lacking NMDA receptors selectively in CA3 pyramidal neurons became more susceptible to kainate-induced seizures. Consistently, mutant mice showed characteristic large EEG spikes associated with multiple unit activities (MUA), suggesting enhanced synchronous firing of CA3 neurons. The electrophysiological balance between fast excitatory and inhibitory synaptic transmission was comparable between control and mutant pyramidal neurons in the hippocampal CA3 region, while the NMDA receptor-slow AHP coupling was diminished in the mutant neurons. In the adult brain, inducible ablation of NMDA receptors in the hippocampal CA3 region by the viral expression vector for Cre recombinase also induced similar large EEG spikes. Furthermore, pharmacological blockade of CA3 NMDA receptors enhanced the susceptibility to kainate-induced seizures. These results raise an intriguing possibility that hippocampal CA3 NMDA receptors may suppress the excitability of the recurrent network as a whole *in vivo* by restricting synchronous firing of CA3 neurons.

**Citation:** Fukushima F, Nakao K, Shinoe T, Fukaya M, Muramatsu S-i, et al. (2009) Ablation of NMDA Receptors Enhances the Excitability of Hippocampal CA3 Neurons. PLoS ONE 4(1): e3993. doi:10.1371/journal.pone.0003993

**Editor:** Frederic Andre Meunier, The University of Queensland, Australia

**Received** September 4, 2008; **Accepted** December 3, 2008; **Published** January 14, 2009



**Funding:** This work was supported in part by Grant-in-Aid for Scientific Research on Priority Areas (Molecular Brain Science) and Global COE Program (Integrative Life Science Based on the Study of Biosignaling Mechanisms) from the Ministry of Education, Culture, Sports, Science and Technology of Japan. F.F. was supported by Japan Society for the Promotion of Science, and S.T. by the 21st Century COE Program, the Ministry of Education, Culture, Sports, Science and Technology of Japan. The funders had no role in study design, data collection and analysis, decision to publish, or preparation of the manuscript.

**Competing Interests:** The authors have declared that no competing interests exist.

* E-mail: mishina@m.u-tokyo.ac.jp

¤a Current address: Division of Molecular and Developmental Biology, Institute of Medical Science, University of Tokyo, Tokyo, Japan,
¤b Current address: Department of Molecular Neuroscience and Pharmaceutical Sciences, Graduate School of Medicine, University of Toyama, Toyama, Japan

## Introduction

Hippocampal CA3 pyramidal neurons form abundant recurrent connections with other CA3 neurons [1,2]. The activity of single pyramidal neurons spreads to other CA3 neurons and this facilitates the rapid synchronization of action-potential firing in CA3 neurons [3]. Synchronized discharges of hippocampal CA3 neurons are supposed to underlie network oscillations [4], memory consolidation [5] and seizure generation [6]. Physiological sharp wave (SPW) activity that occurs during slow-wave sleep and behavioral immobility is dependent on synchronous discharges by population of CA3 pyramidal neurons [7,8]. Synchronized CA3 activity may also contribute to the pathological EEG pattern, known as an interictal spike, which indicates a propensity for temporal lobe seizures [6].

NMDA receptors play key roles in synaptic plasticity and memory [9]. In the CA3 network, NMDA receptors are abundant at the commissural/associational synapses but scarce at the mossy fiber synapses [10]. Thus, the CA3 recurrent network is under the control of NMDA receptors. NMDA receptors in the hippocampal CA3 region are implied in rapid acquisition and recall of associative memory as well as paired associate learning [11–13]. On the other hand, studies with hippocampal slices showed that the synchronous network activity induces NMDA receptor-dependent LTP of CA3 recurrent synapses [14] and that stimuli that induced NMDA receptor-dependent LTP in the CA3 region generated sharp wave-like synchronous network activity [15]. These *in vitro* observations raised the hypothesis that the NMDA receptor-mediated LTP contributes to the generation of synchronous network activity. Here, we generated hippocampal CA3 pyramidal neuron-specific NMDA receptor mutant mice on the pure C57BL/6N genetic background. The ablation of hippocampal CA3 NMDA receptors resulted in the enhancement of the susceptibility to kainate-induced seizure and the emergence of characteristic large EEG spikes. We also showed that the virus-mediated ablation of hippocampal CA3 NMDA receptors in the

adult mice generated characteristic large EEG spikes and that pharmacological blockade of CA3 NMDA receptors enhanced the susceptibility to kainate-induced seizures. These results raise an intriguing possibility that NMDA receptors may control negatively the excitability of the hippocampal CA3 recurrent network as a whole *in vivo*.

## Methods

### Generation of mice

Genomic DNA carrying the exon 11 to 22 of the *GluRζ1* gene was isolated by screening a bacterial artificial chromosome (BAC) library prepared from the C57BL/6 strain (Incyte Genomics) with the 2.2 kb-*Eco*RI fragment from pBKSAζ1 [16]. The 13.3-kb *Eco*RI-*Xba*I fragment of the BAC clone was used for construction of the targeting vector. The *loxP* site was inserted into the *Bam*HI site between exon 18 and 19, and the 1.8-kb DNA fragment carrying the *loxP* sequence and *Pgk-1* promoter-driven neomycin phosphotransferase gene (*neo*) flanked by two Flp recognition target (*frt*) sites into the *Spe*I site between exon 20 and 21. Endogenous *Eco*RI site at the 5′ end of 13.3-kb *Eco*RI-*Xba*I genomic fragment was replaced with *Not*I site and an exogenous *Eco*RI site was inserted between the second *loxP* site and *neo* gene. The targeting vector pζ1TV was composed of the 14.8-kb *Not*I-*Xba*I fragment, MC1 promoter-driven diphteria toxin gene derived from pMC1DTpA and pBluescript II SK(+) [17]. The targeting vector was linearized by *Not*I and electroporated into ES cells derived from the C57BL/6N strain [18,19]. Recombinant clones were identified by Southern blot analysis of *Eco*RI-digested genomic DNA using 284-bp fragment amplified with primers 5′-ATAGAGAAAGACATGGGGC-3′ and 5′-TGCTACTGTGCAGGAAGTG-3′ from pζ1TV, the 0.6 kb *Pst*I fragment from pLFNeo [20], and the 1.1-kb *Xho*I–*Eco*RI fragment from the BAC clone as 5′ inner, neo, and 3′ outer probes, respectively. The $GluR\zeta1^{flox}$ allele was also identified by PCR using primers 5′-GCAGTGAGGCTCACACAGGCCTGAAGACTA-3′ and 5′-AGTGAACTCGGATCCTGACCATTGGCCACT-3′. Chimeric mice production and elimination of the *neo* gene from the genome through Flp/frt-mediated excision were carried out essentially as described [18–20].

GluRγ1-Cre mice were obtained by inserting the *cre* gene in the translational initiation site of the *GluRγ1* gene in frame using ES cells derived from the C57BL/6N strain [19]. The 1.8-kb DNA fragment, which carried the polyadenylation signal sequence and *pgk-1* promoter-driven *neo* gene flanked by two *frt* sites [20], was inserted into the downstream of the *cre* gene. $GluR\zeta1^{+/flox}$ mice were crossed with GluRγ1-Cre mice to yield $GluR\gamma1^{+/cre}$; $GluR\zeta1^{flox/flox}$ mice. The $GluR\gamma1^{+/cre}$ allele was identified by PCR using primers 5′-AACTGCAGTCTTGCATGCTCTCTGGAGCC-3′, 5′-GGAGCGGAGACACGGGGCAT-3′ and 5′-TTGCCCCTGTTTCACTATCC-3′. Cre recombinase-mediated NMDA receptor ablation is hippocampal CA3 pyramidal neuron-specific in $GluR\gamma1^{+/cre}$; $GluR\zeta1^{flox/flox}$ mice (Fig. 1). It is unknown why the *GluRγ1* promoter-driven Cre expression does not exactly follow the expression pattern of GluRγ1 [21]. The insertion of the *pgk-1* promoter-driven *neo* gene and the polyadenylation signal sequence together may affect the Cre expression pattern since the elimination of the *neo* gene through Flp-mediated recombination altered the expression pattern.

All animal procedures were approved by the Animal Care and the Use Committee of Graduate School of Medicine, the University of Tokyo (Approval # 1721T062). Mice were fed *ad libitum* with standard laboratory chow and water in standard animal cages under a 12 h light/dark cycle.

### AAV-Cre vector

We employed AAV to deliver Cre recombinase since AAV is safe, non-pathogenic, non-inflammatory and extremely stable stable [22,23]. AAV-Cre or AAV-EGFP vector contains an expression cassette consisting of a human cytomegalovirus immediate-early promoter (CMV promoter), followed by the human growth hormone first intron, cDNA of Cre recombinase with a nuclear localization signal or the enhanced green fluorescence protein (EGFP), and simian virus 40 polyadenylation signal sequence (SV40 polyA), between the inverted terminal repeats (ITR) of the AAV-2 genome. The two helper plasmids, pAAV-RC and pHelper (Agilent Technologies, Santa Clara, California), harbor the AAV *rep* and *cap* genes, and the *E2A*, *E4*, and *VA RNA* genes of the adenovirus genome, respectively. HEK293 cells were cotransfected by the calcium phosphate coprecipitation method with the vector plasmid, pAAV-RC, and pHelper. AAV vectors were then harvested and purified by two sequential continuous iodoxale ultracentrifugations. The vector titer was determined by quantitative DNA dot-blot hybridization or quantitative PCR of DNase-I-treated vector stocks. Before administration, AAV vectors were diluted in phosphate-buffered saline to $5–8\times10^{10}$ genome copies/μl. A glass micropipette was inserted into the hippocampal CA3 region of ketamine-anesthetized mice (AP, L, V = −1.2, ±1.2, +2.0; −1.7, ±2.0, +2.1; −2.2, ±2.5, +2.4; −2.7, ±3.2, +3.5; −3.2, ±2.5, +4.0). Two minutes after the insertion, 1.0 μl of a virus solution or vehicle was injected at a constant flow rate of 16.6 nl/min, and the glass micropipette was left in this configuration for an additional 2 min, to prevent reflux of the injected material along the injection track, before being slowly retracted. AAV spread 0.5–0.7 mm both rostrodorsally and laterally. For every injected animal, the limit of the infected region was verified by immunohistochemistry for Cre recombinase or GluRζ1.

### Immunological analysis

Immunohistochemistry was done as described [24] using antibodies against VGluT2 (guinea pig) [25], Calbindin (rabbit) [26], PSD-95 (rabbit) [27], GluRα1 (rabbit) [28], GAD (guinea pig) [29], and Cre recombinase (1:1000; rabbit; Novagen). Immunobloting analyses in whole-brain homogenate were carried out using antibodies for GluRζ1 (rabbit) [30], and neuron-specific enolase (1:4000; Chemicon) and chemiluminescense (Amersham Biosciences).

### Golgi staining

Coronal brain sections (2 mm) were immersed for 4 days in a solution composed of 5% glutaraldehyde (Wako) and 2% $K_2Cr_2O_7$ (Sigma) and then transferred to a 0.75% solution of $AgNO_3$ (Sigma) for further 4 days. The treated brain was sectioned (100 μm), dehydrated and mounted on glass slides.

### Morphology of AAV-EGFP infected CA3 neurons

AAV-EGFP vector was delivered into the hippocampal CA3 region of ketamine-anesthetized control and mutant mice of 8 weeks old. Fourteen days later, fixed coronal brain sections (150 μm) were prepared. Neurons were examined with a Leica SP-5 confocal laser scanning microscope. Optical sections were collected at intervals of 0.15 μm and averaged 16 times using a 100×objective (N.A. 1.4). The distance between axonal varicosities was measured from 50 μm-portions of CA3 axons within the CA3 stratum radiatum [31]. For spine analysis, only spines on clearly visible tertiary apical and basal branches were imaged. During the quantitation of the spine density, putative spines in the

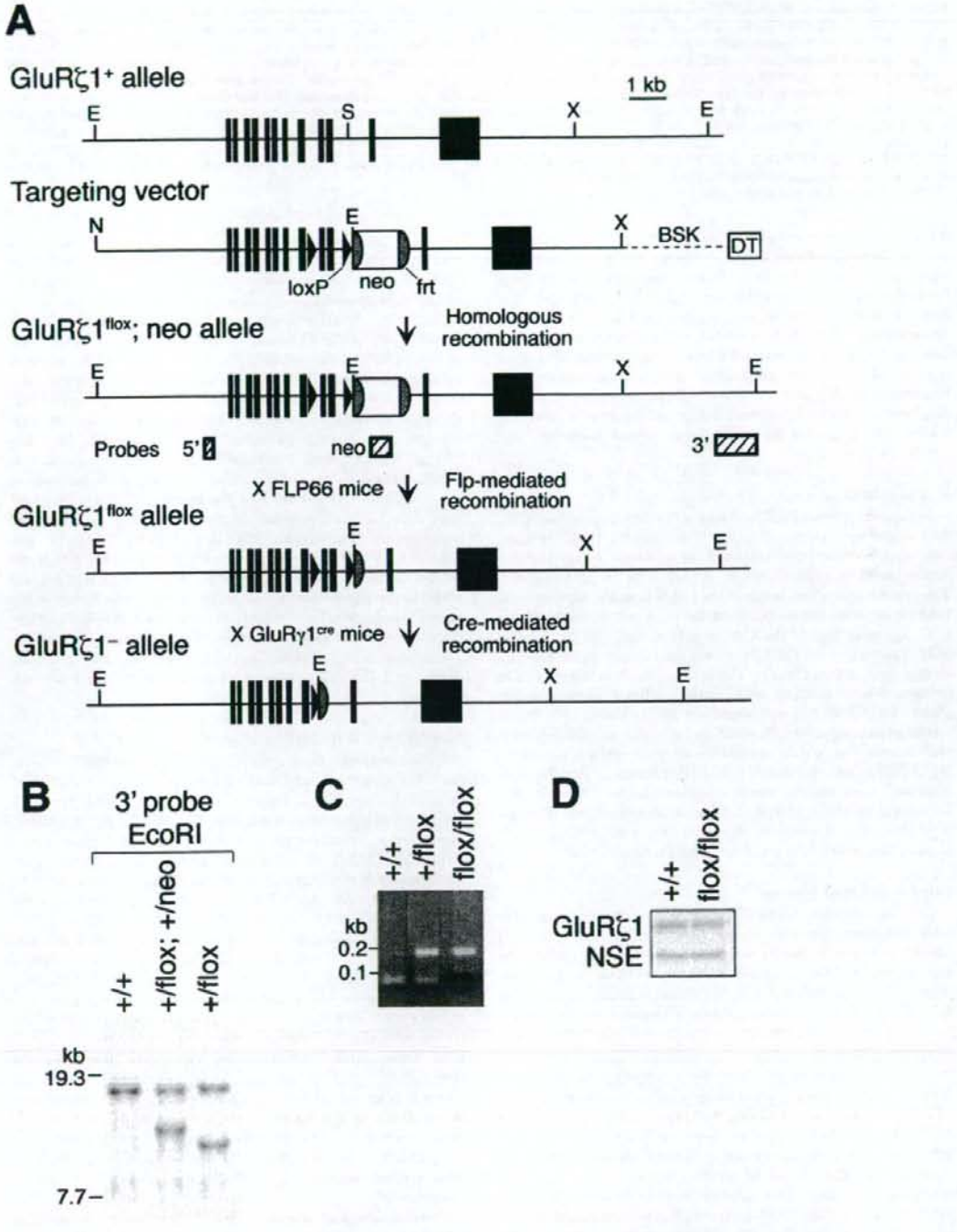
A
GluRζ1+ allele
1 kb
E
S
X
E
Targeting vector
N
E
X
BSK
DT
loxP
neo
frt
GluRζ1flox; neo allele
Homologous recombination
E
E
X
E
Probes 5'
neo
3'
X FLP66 mice
Flp-mediated recombination
GluRζ1flox allele
E
E
X
E
X GluRγ1cre mice
Cre-mediated recombination
GluRζ1− allele
E
E
X
E
B
3' probe EcoRI
+/+
+/flox; +/neo
+/flox
kb
19.3
7.7
C
+/+
+/flox
flox/flox
kb
0.2
0.1
D
+/+
flox/flox
GluRζ1
NSE